# Design of a 600 W half-bridge LLC converter using 600 V CoolMOS™ CFD7

Authors: Francesco Di Domenico
Alois Steiner

## About this document

### Scope and purpose

This application note (AN) will describe the design and performance of a 600 W LLC demo board. This is a high-performance example with a complete Infineon solution, including HV and LV power MOSFETs, controllers and drivers. This document demonstrates a very effective way to design the HV DC-DC isolation stage of a server PSU fulfilling the 80Plus® Titanium standard.

Besides design information and documentation for the LLC converter, the reader will receive additional information regarding how the 600 V CoolMOS™ CFD7 superjunction MOSFET behaves in this LLC demo board and the benefits that will be achieved. The AN also provides suggestions on how to develop LLC converters in similar power ranges adapted to specific requirements.

### Intended audience

This document is intended for design engineers who wish to evaluate high-performance alternative topologies for medium- to high-power SMPS converters, and develop an understanding of the design process. Also, how to apply the somewhat complex LLC design methods to their specific system applications.

## Table of contents

**Table of contents** ..... **1**
**1 Introduction** ..... **3**
**2 HB LLC converter principles of operation** ..... **5**
2.1 Tank configuration and operational modes ..... 5
2.2 Analysis of the basic tank characteristics using FHA ..... 8
2.3 Tank Q values and m inductance ratio: system implications ..... 9
2.4 Benefits of split capacitor $C_r$ ..... 9
2.5 SR (SR) concepts for LLC ..... 10
**3 LLC design methodologies for specific application requirements** ..... **12**
3.1 Input design data ..... 12
3.2 Gain curve ..... 13
3.3 Suggested FHA optimization process ..... 14
3.4 Notes on the selection of the inductance factor (m) ..... 14
3.5 Resonant components calculation ..... 15
3.6 ZVS behavior: energy and time considerations ..... 15
3.6.1 Energy-related equations ..... 16
3.6.2 Time-related equations ..... 16
3.7 Main transformer design ..... 17
3.8 Resonant choke design ..... 20
3.9 SR stage ..... 20

Table of contents

**4 Board description ..... 22**
4.1 General overview ..... 22
4.2 Infineon components used in the board ..... 23
4.2.1 Primary HV MOSFETs 600 V CoolMOS™ CFD7 ..... 23
4.2.2 LLC analog controller ICE2HS01G ..... 23
4.2.3 HB gate driver 2EDL05N06PFG ..... 24
4.2.4 Advanced dual-channel gate driver 2EDN7524F ..... 24
4.2.5 Bias QR flyback controller ICE2QR2280Z ..... 25
4.2.6 SR MOSFETs OptiMOS™ BSC010N04LS ..... 25
4.3 Board schematics ..... 26
4.3.1 Main board schematic ..... 26
4.3.2 Controller board schematic ..... 27
4.3.3 Bias board schematic ..... 28
4.4 Critical LLC operation – hard commutation ..... 29
4.5 ZVS behavior analysis ..... 31
4.6 Burst mode operation ..... 31
4.7 Efficiency ..... 32
4.7.1 80Plus® Titanium efficiency target ..... 32
4.7.2 Losses breakdown ..... 34
**5 Conclusion ..... 36**
**6 Test/power-up procedure ..... 37**
**7 Useful materials and links ..... 39**
**8 References ..... 40**
**9 List of abbreviations ..... 41**
**Revision history ..... 42**

# 1 Introduction

The reduction in size of power converters by increasing switching frequency and reducing magnetic component size is a goal that has been pursued for decades. The development of resonant converters with ZVS has been a cornerstone of this effort, but for a long time they have been considered as a way to “make good power solutions from mediocre semiconductors”, in fact limiting their usage. Moreover, with the advent of CoolMOS™ high-performance silicon switches based on the superjunction (SJ) concept, the improvements in Figure of Merit (FOM) reduced the need to use resonant topologies for many years. Now, the industry requirements for highly efficient converter performance, which drove a trend toward resonant-switching square-wave converters, such as the Phase-Shift Full-Bridge (PSFB) converter, are creating a need for a closer look at the somewhat more difficult-to-design multi-resonant LLC converter.

Classically, fully resonant converters have had a nominal disadvantage in conduction losses compared with soft-switching square-wave converters such as the PSFB, due to the difference in peak versus RMS current for sinusoidal current waveshapes versus trapezoidal. However, with the advent of the multi-resonant converter, it is possible with modern MOSFETs and their excellent FOM to achieve better optimized results with the LLC converter. This is in large part due to the fact that the square-wave converter is optimized at maximum duty cycle, which is only achieved at low-line condition. Hence, to provide operational capability with typical Power Factor Correction (PFC) front ends, and some converter hold-up time capability, they will typically need to be optimized for DC input as low as 325 V or 300 V, while they will normally operate at 380 V with a less favorable crest factor and higher net RMS current.

In contrast, an LLC converter can be optimized for the nominal DC input voltage, and use the boost-up mode below the main resonance to achieve low-line regulation with proper design. Combine this with a favorable silicon Bill of Materials (BOM) situation – compared with a PSFB topology – and the proper design approach, and a high-performance converter is within easy reach.

In Figure 1, there is a synthetic comparison of several FOM metrics based on cost and performance between the PSFB converter and the Half-Bridge (HB) LLC.

It can be seen that the first topology (blue arrows) retains some important features, especially in controllability and flexibility with wide output regulation range, but the HB LLC (red arrows) provides some very important benefits in a modern SMPS design, including reduced BOM, easier ZVS and better Synchronous Rectification (SR).

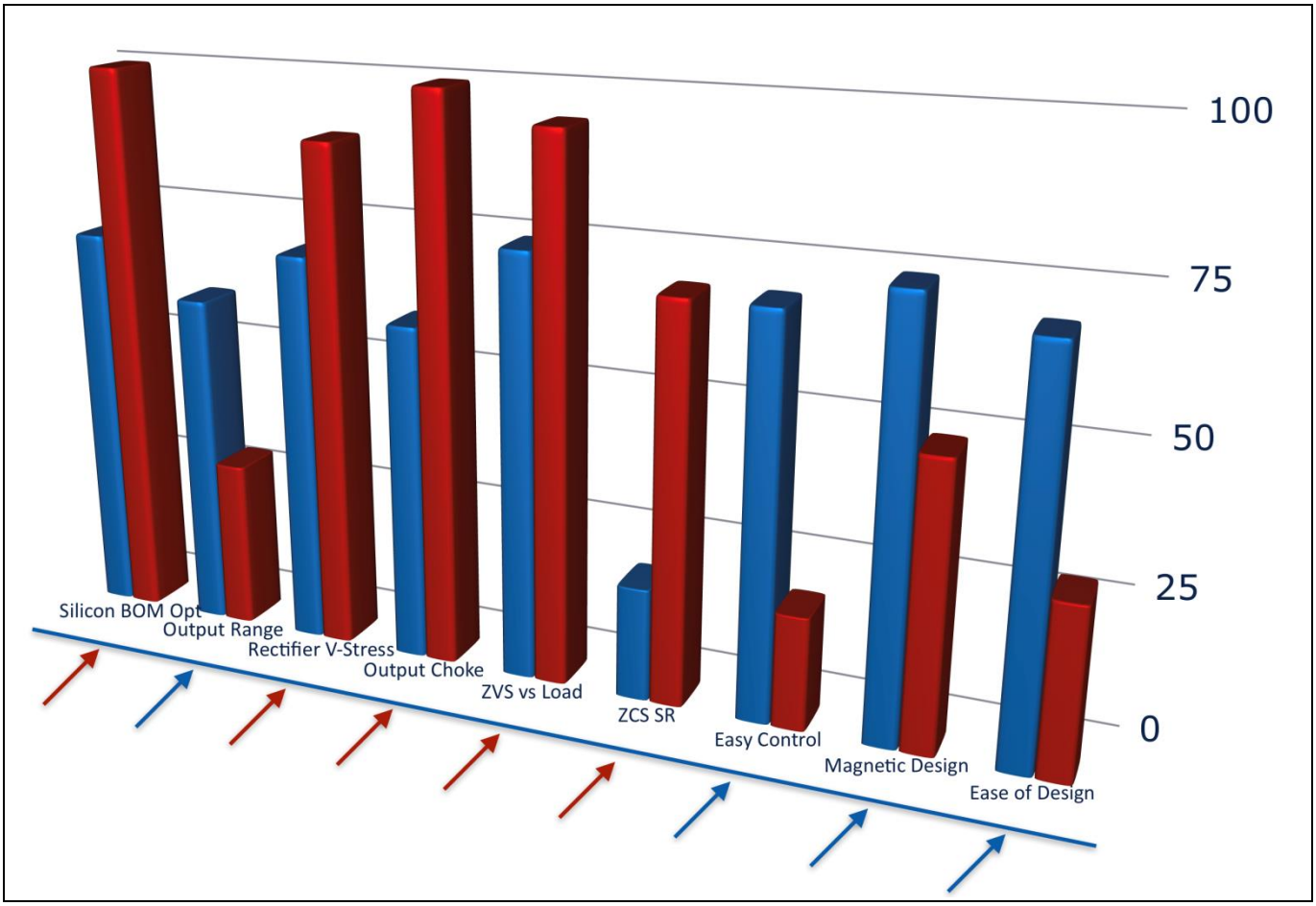


**Figure 1 Comparison of several FOM metrics based on cost and performance between the PSFB converter and the HB LLC**

The principles of operation for the LLC converter will be examined in the next section, and the main tank design concepts reviewed. This will be followed by detailed design methodologies using First Harmonic Approximation (FHA) and supplemented by exact design concepts.

The scope of this document is to describe the details of an analog-controlled 600 W HB LLC demo board fully designed using Infineon products. (Order information in ISAR: EVAL_600W_12V_LLC_CFD7.)

The target efficiency of this design is determined according to the need to fulfill (for the complete PSU) the 80Plus® Titanium standard, meaning certain minimum efficiency requirements for the HV DC-DC stage are fixed at 10 percent, 20 percent, 50 percent and 100 percent load conditions.

# 2 HB LLC converter principles of operation

The typical modes of operation of the LLC converter will be discussed in this chapter using an initial description of the concept behind FHA. The reasoning behind the basic configuration of the resonant tank will be introduced shortly. Finally, the concepts and challenges for successful implementation of SR will be outlined.

The most important concepts are referred to here, in order to better understand the design considerations.

## 2.1 Tank configuration and operational modes

The principal schematic of an HB LLC converter is shown in Figure 2.

$C_r$, $L_r$ and $L_m$ represent the “resonant tank”. Together with the main transformer, they are the key components in the LLC design.

The primary HB and the output rectification are the other two stages to be defined.

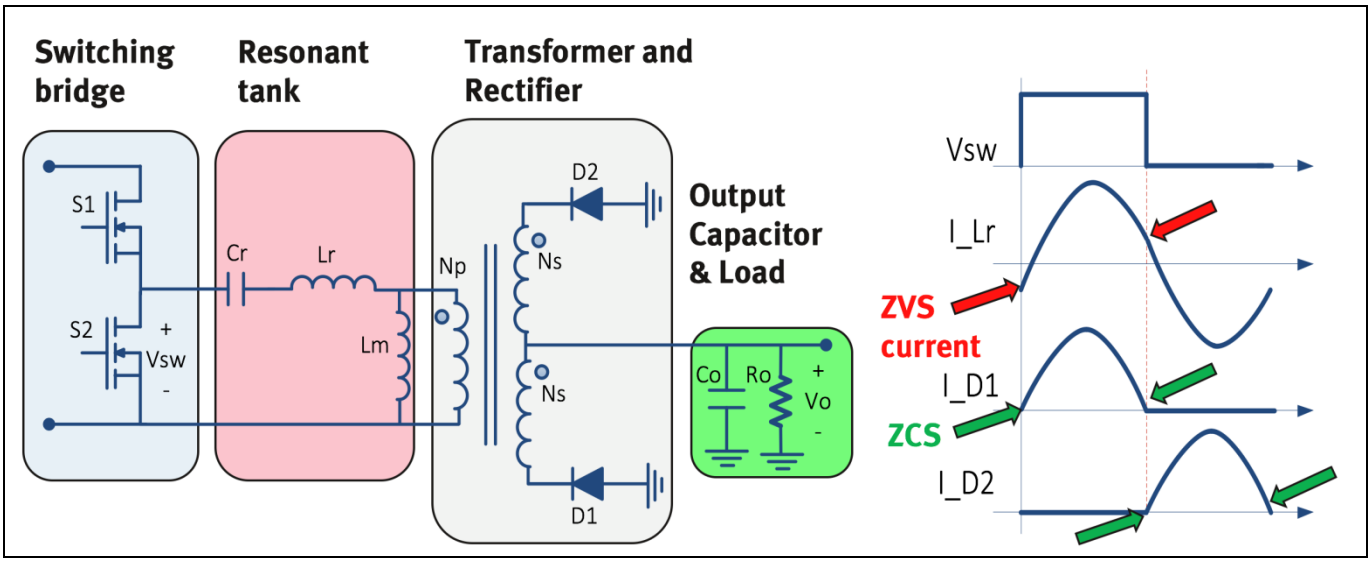


**Figure 2 Principle schematic of an HB LLC converter**

The LLC is a resonant converter that operates with frequency modulation instead of the traditional PWM approach to power conversion.

Figures 3, 4, 5 and 6 explain the fundamental operating mode of an HB LLC converter in a graphic format.

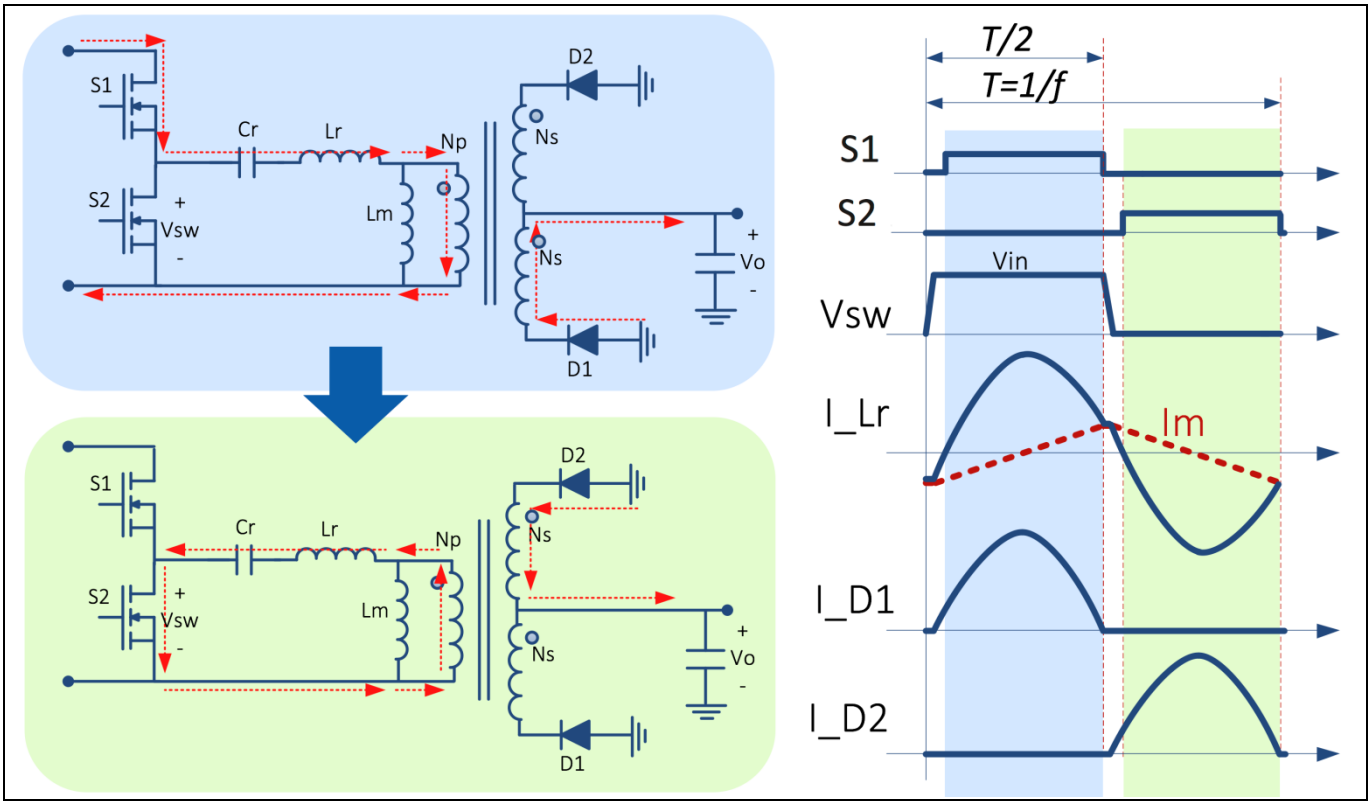


**Figure 3** **Fully resonant operating mode, at the resonant point for $C_r$ and $L_r$, with near-ZCS turn-off of the primary-side MOSFETs**

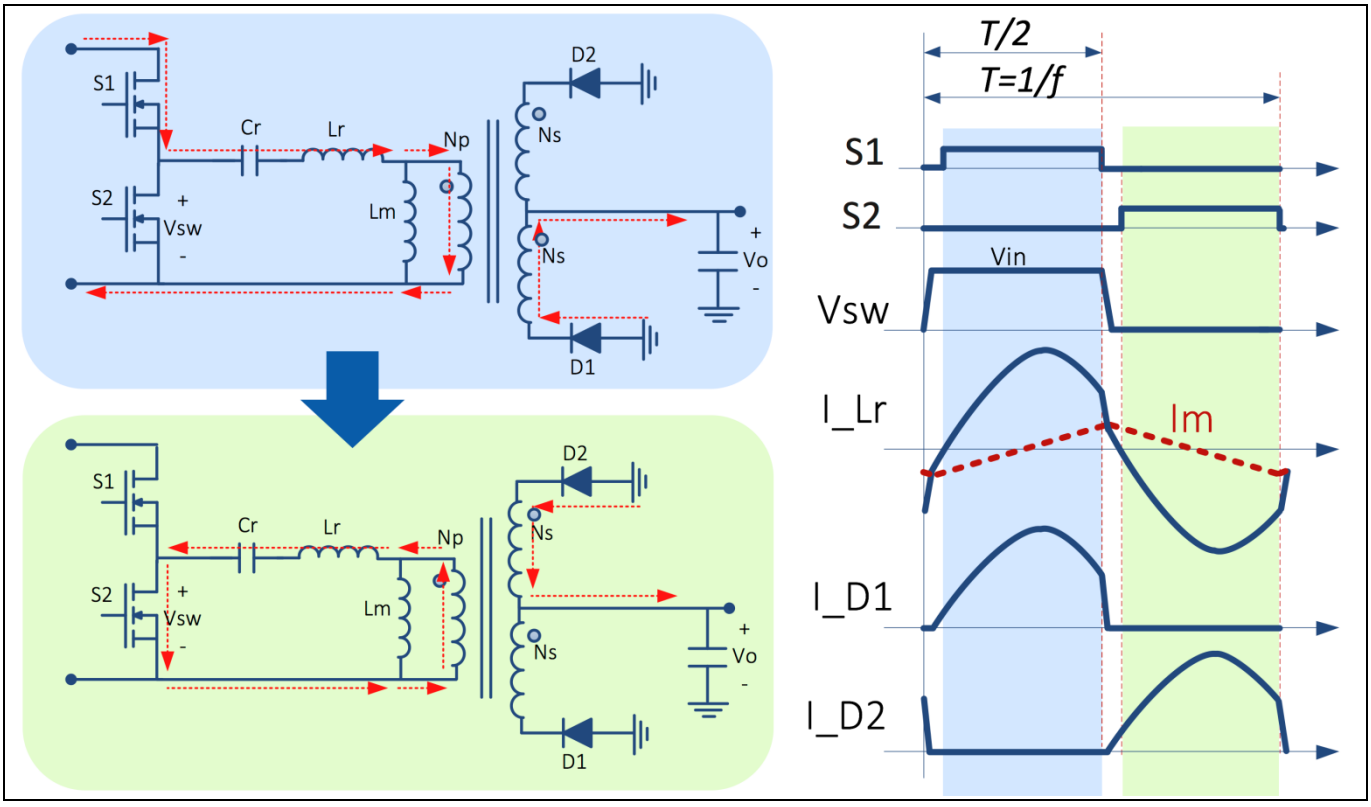


**Figure 4** **Over resonant operation, above $C_r$-$L_r$ resonance, for both half-cycles, showing tank current waveforms and non-ZCS turn-off of the primary-side MOSFETs**

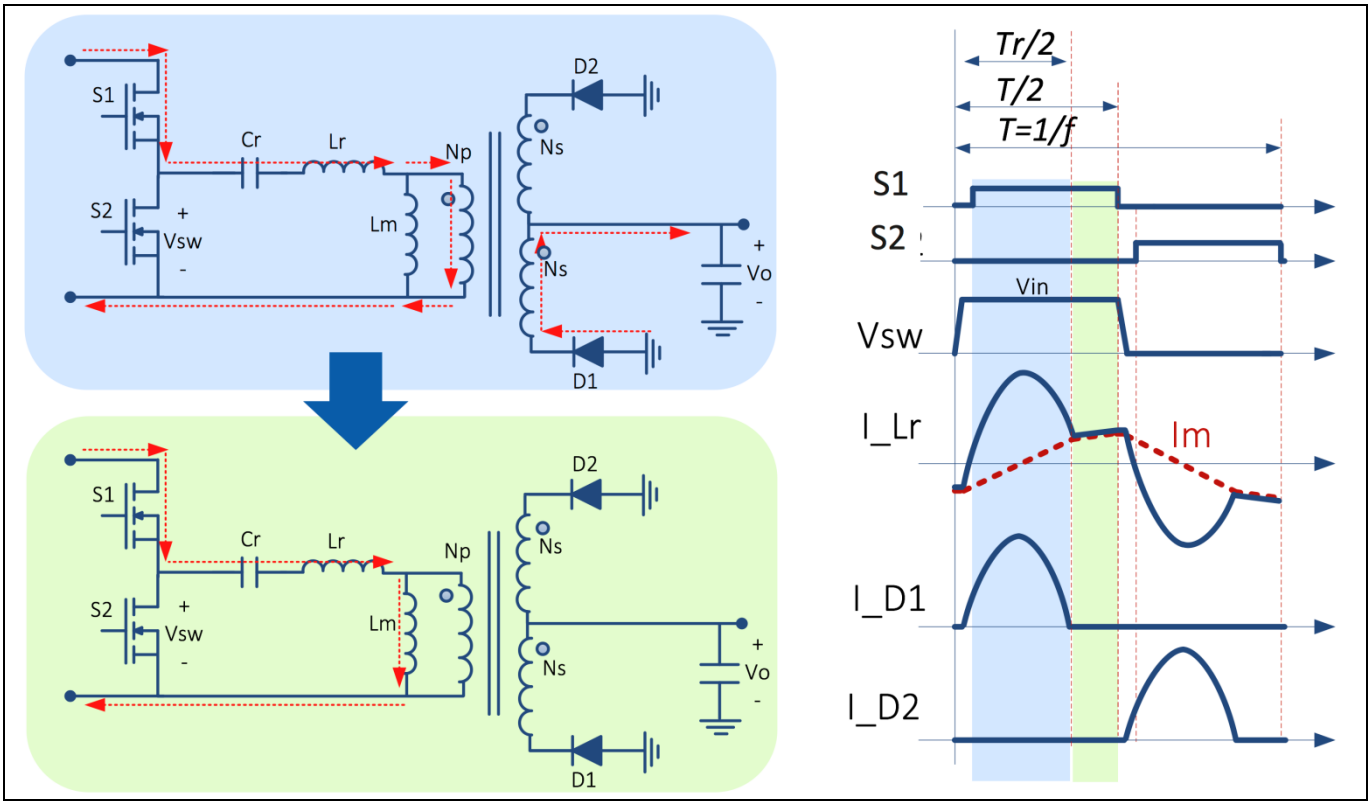


**Figure 5** **Under resonant Discontinuous Current Mode (DCM) operation, (between the resonant point of $C_r$ and $L_r$ vs the resonant point of $C_r$ and $L_r$+$L_m$) half-cycle 1**

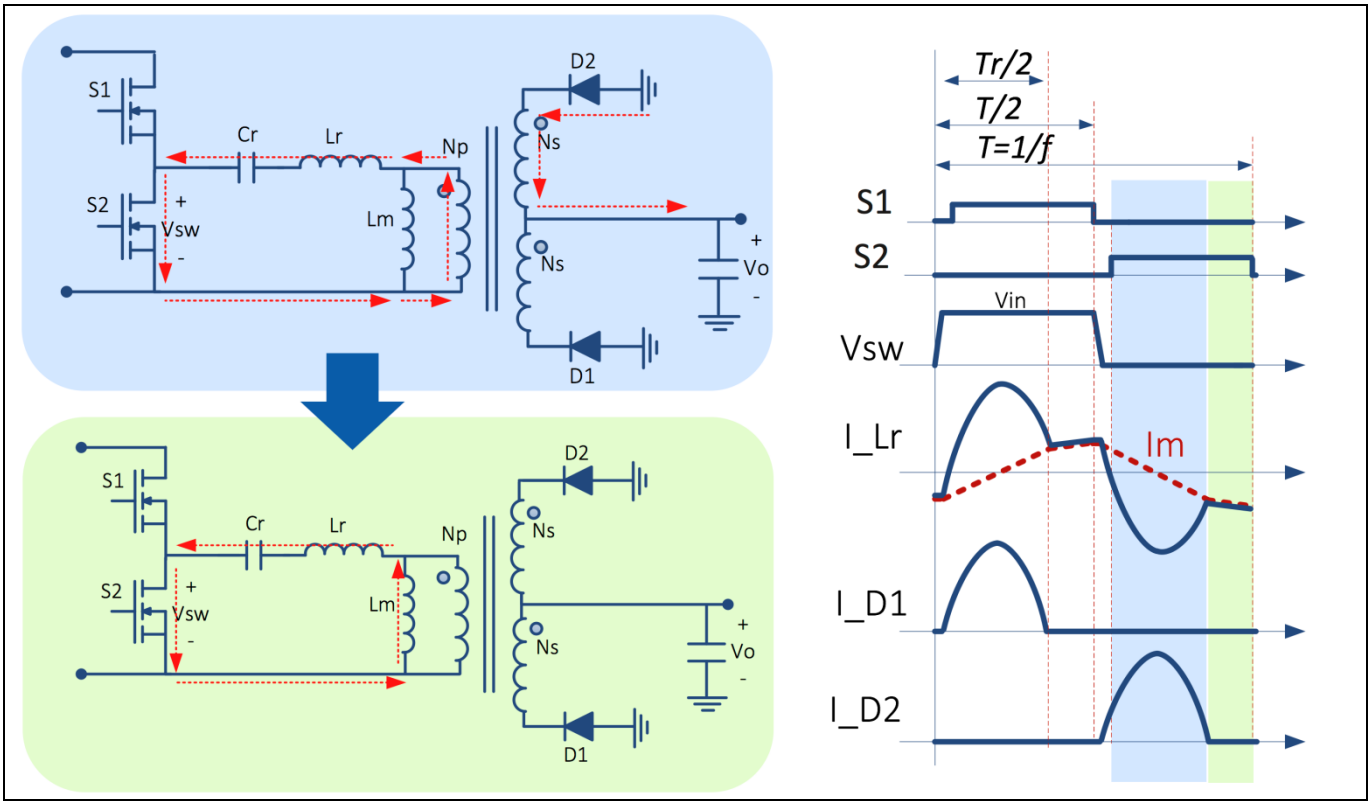


**Figure 6** **Under resonant DCM mode operation, (between the resonant point of $C_r$ and $L_r$ vs the resonant point of $C_r$ and $L_r$+$L_m$) half-cycle 2**

## 2.2 Analysis of the basic tank characteristics using FHA

The starting point in a resonant converter design is the definition of an energy transfer function, which can be seen as a voltage gain function, or a mathematical relationship between the input and output voltages of the converter. Trying to obtain this function in an exact way involves several non-linear circuit behaviors governed by complex equations. However, under the assumption that the LLC operates in the vicinity of the series resonant frequency, important simplifications can be introduced.

In fact, under this assumption, the current circulating in the resonant tank can be considered purely sinusoidal, ignoring all higher-order harmonics: this is the so-called First Harmonic Approximation (FHA) method, which is the most common approach to the design of an LLC converter.

In the FHA, the voltage gain is calculated with reference to the equivalent resonant circuit shown in Figure 7.

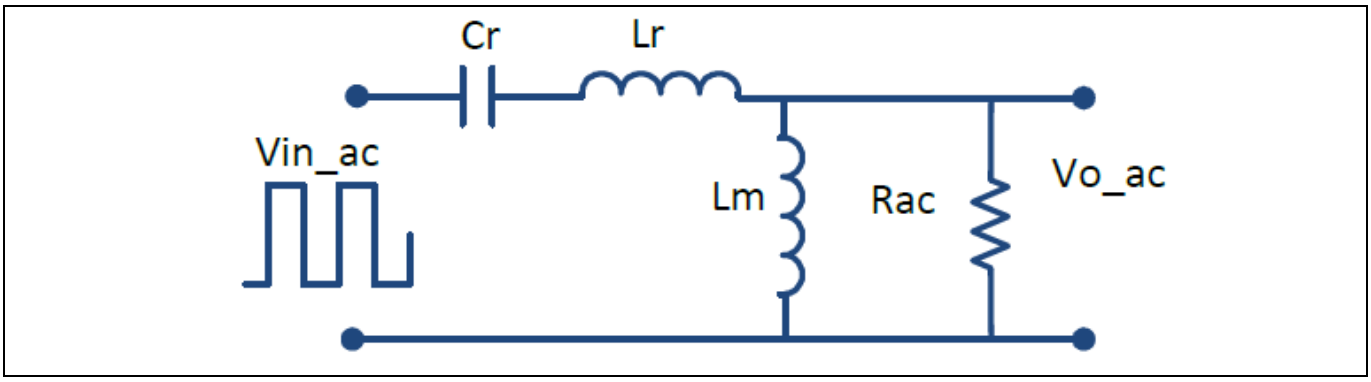


**Figure 7 FHA equivalent resonant circuit**

The mathematical expression for the gain (K) is given in terms of a normalized resonant frequency $F_x$:

$$K(Q,m,Fx)=\left|\frac{V_{o_ac}(s)}{V_{in_ac}(s)}\right|=\frac{F_x^2(m-1)}{\sqrt{(m\cdot F_x^2-1)^2+F_x^2\cdot(F_x^2-1)^2\cdot(m-1)^2\cdot Q^2}} \quad (1)$$

Where:

$$m=\frac{Lr+Lm}{Lr};\qquad fr=\frac{1}{\sqrt{Lr\cdot Cr}};\qquad Fx=\frac{fs}{fr};\qquad Rac=\frac{8}{\pi^2}\cdot\frac{Np^2}{Ns^2}\cdot Ro;\qquad Q=\frac{\sqrt{Lr/Cr}}{Rac}; \quad (2)$$

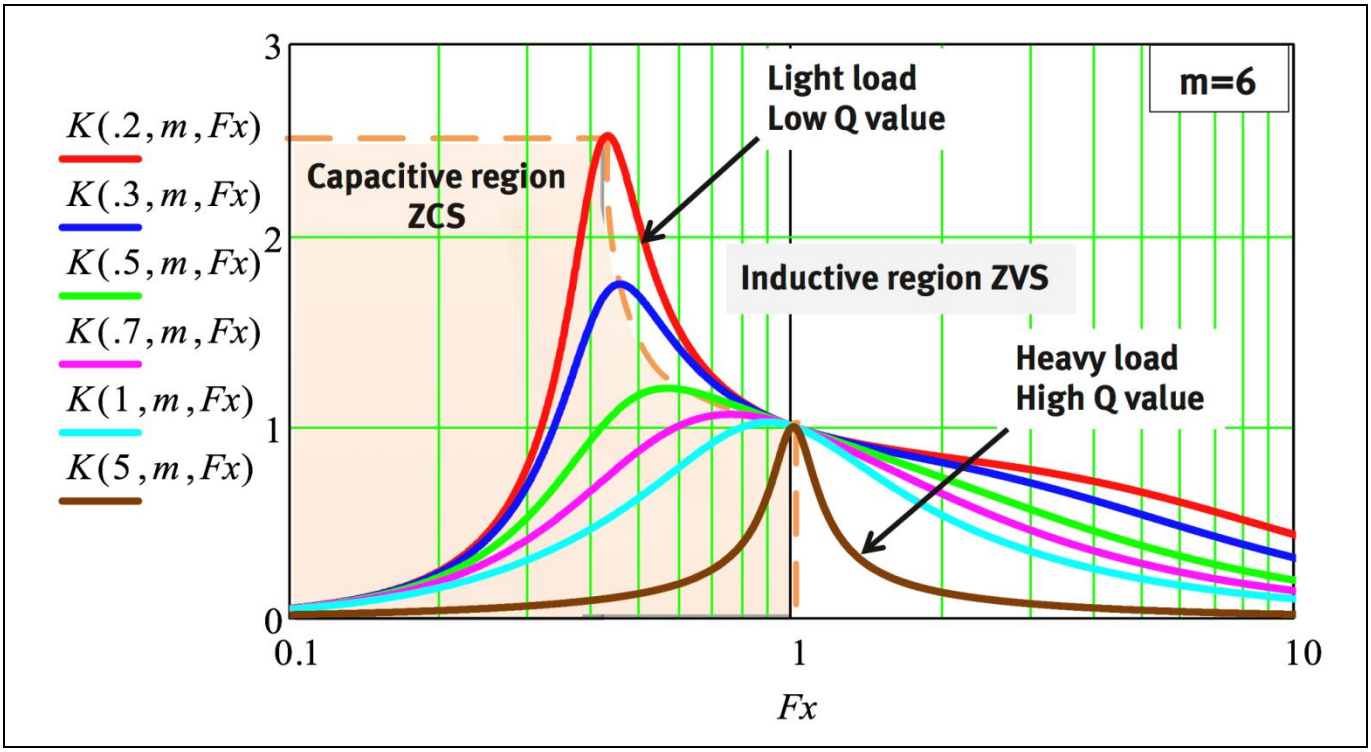


**Figure 8 Family of Q curves for a fixed m inductance ratio of 6**

## 2.3 Tank Q values and m inductance ratio: system implications

The resonant tank gain K can be plotted as a function of the normalized driving frequency $F_x$ for different values of the quality factor Q and any single value of the inductance ratio factor m.

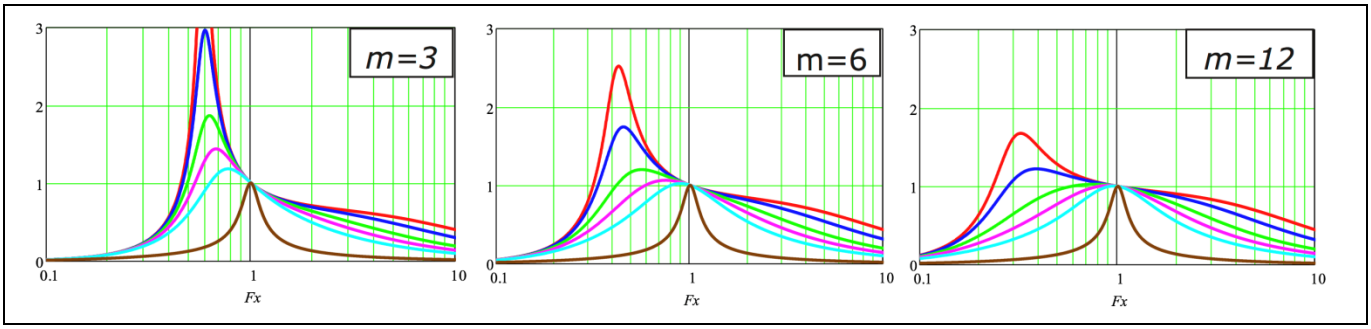


**Figure 9 Family of Q curves for m inductance ratios of 3, 6 and 12**

## 2.4 Benefits of split capacitor $C_r$

The design described in this document uses the configuration shown in Figure 10, typically known as the “split resonant capacitor technique”. This solution provides a couple of important benefits.

The first benefit is the reduction of the AC current stress on the resonant and input bulk capacitors, with consequent relaxed AC current requirements on those components, thereby achieving cost reduction and extended lifetime.

The second benefit involves the often-critical LLC start-up sequence.

In fact, the split capacitor technique provides the possibility of charging the resonant capacitance simultaneously to the input bulk cap, thus reducing the required charging time. In fact, until the resonant capacitor is completely charged, the transformer is not driven symmetrically, so there is a significant difference in the up and down slopes of the resonant current and the current may not reverse in a switching half-cycle. This condition could create a potentially damaging condition where a MOSFET is turned on while the body diode of the other HB MOSFET is conducting. This is the condition known as “hard commutation on the conducting body diode”, which submits the turning-off device to heavy stress. This may happen for several cycles at converter start-up.

Using the split resonant capacitor technique, the risk of hard commutation is significantly reduced when the HV DC-DC converter is powered up in a relatively short time after the input bulk capacitor has been charged to the DC link voltage.

It should be noted that this technique can reduce the possibility of hard commutation, but does not guarantee 100 percent prevention.

A safe and reliable operation at start-up is only possible through a proper control algorithm and HV MOSFET driving technique, along with a power device with a rugged body diode.

For further detail on this topic, please refer to paragraph 4.4 of this document, and [4].

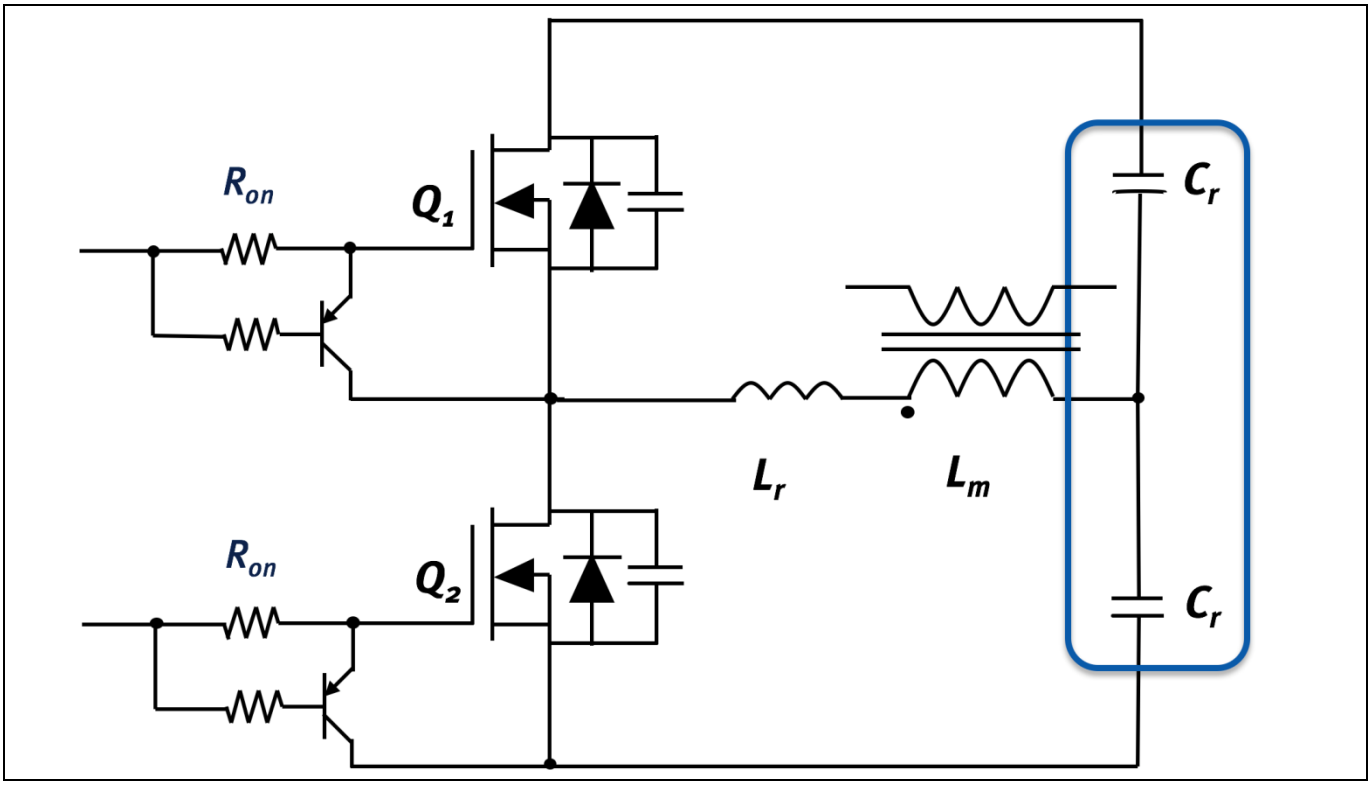


**Figure 10 Rearranging the resonant capacitor into a split capacitor HB configuration**

## 2.5 SR (SR) concepts for LLC

Figure 11 briefly summarizes the technique of managing SR in an HB LLC converter.

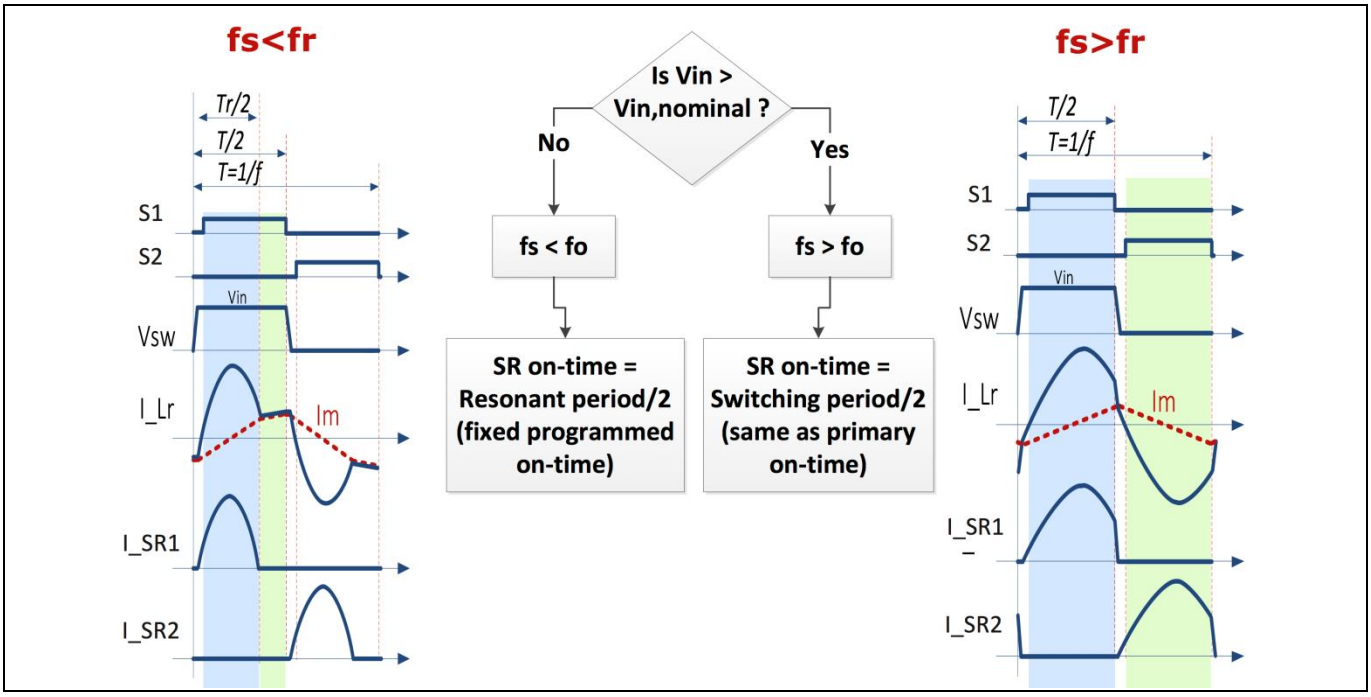


**Figure 11 SR in an HB LLC converter**

# 3 LLC design methodologies for specific application requirements

An optimization procedure for the selection of the main LLC parameters, both for the FHA method and using exact calculation or simulation, is shown in the next section. The goal is to achieve the best performance while fulfilling input and output regulation requirements.

At the same time, ZVS operation of the primary HB MOSFETs must be ensured in order to get the full benefit of the soft-switching behavior, especially at light load.

## 3.1 Input design data

Table 1 gives an overview of the major design parameters.

**Table 1 Design parameters**

| Description | Minimum | Nominal | Maximum |
|---|---|---|---|
| Input voltage | 350 V DC | 380 V DC | 410 V DC |
| Output voltage | 11.9 V DC | 12 V DC | 12.1 V DC |
| Output power | | | 600 W |
| Efficiency at 50 percent $P_{max}$ | 97.4 percent | | |
| Switching frequency | 90 kHz | 150 kHz | 250 kHz |
| Dynamic output voltage regulation (0–90 percent load-step) | | | Maximum overshoot = 0.1 V<br>Maximum undershoot = 0.3 V |
| $V_{out_ripple}$ | | | 150 $mV_{pk-pk}$ |

From the table above, the first important design parameters can be derived:

Main transformer turn ratio

$$n = \frac{N_p}{N_s} = \frac{V_{in_nom}}{2 \cdot V_{out_nom}} \approx 16 \quad (3)$$

Minimum needed gain

$$K_{\min}(Q, m, F_x) = \frac{n \cdot V_{o_\min}}{V_{in_\max}/2} \approx 0.95 \quad (4)$$

Maximum needed gain

$$K_{\max}(Q, m, F_x) = \frac{n \cdot V_{o_\max}}{V_{in_\min}/2} \approx 1.08 \quad (5)$$

## 3.2 Gain curve

The resulting gain curves in Figure 12, for loads between 10 percent and 100 percent of $P_{max}$, are shown in the following plot:

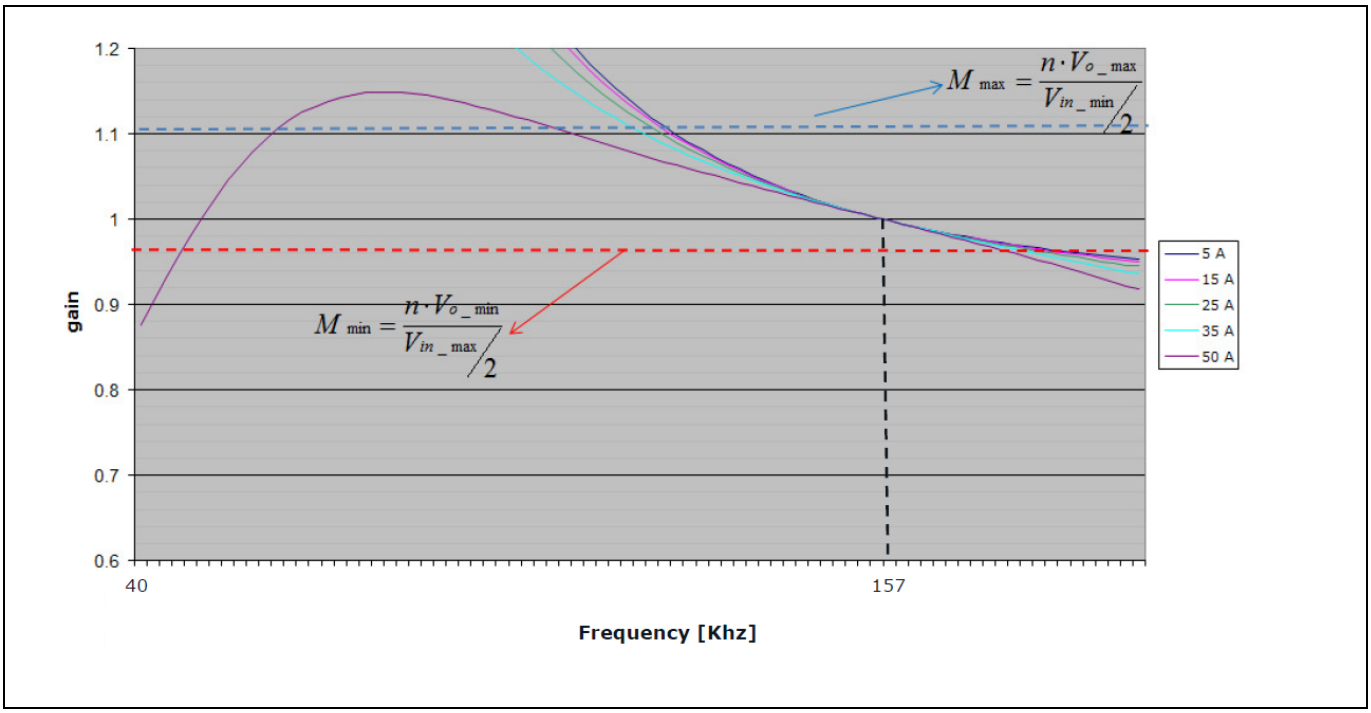


**Figure 12 Gain curve**

Both the $M_{min}$ and $M_{max}$ limits cross all the gain curves of our LLC converter, meaning that the input/output regulation is fully achieved in the specified ranges.

## 3.3 Suggested FHA optimization process

Figure 13 is a flowchart that shows all the steps in the design of an HB LLC converter.

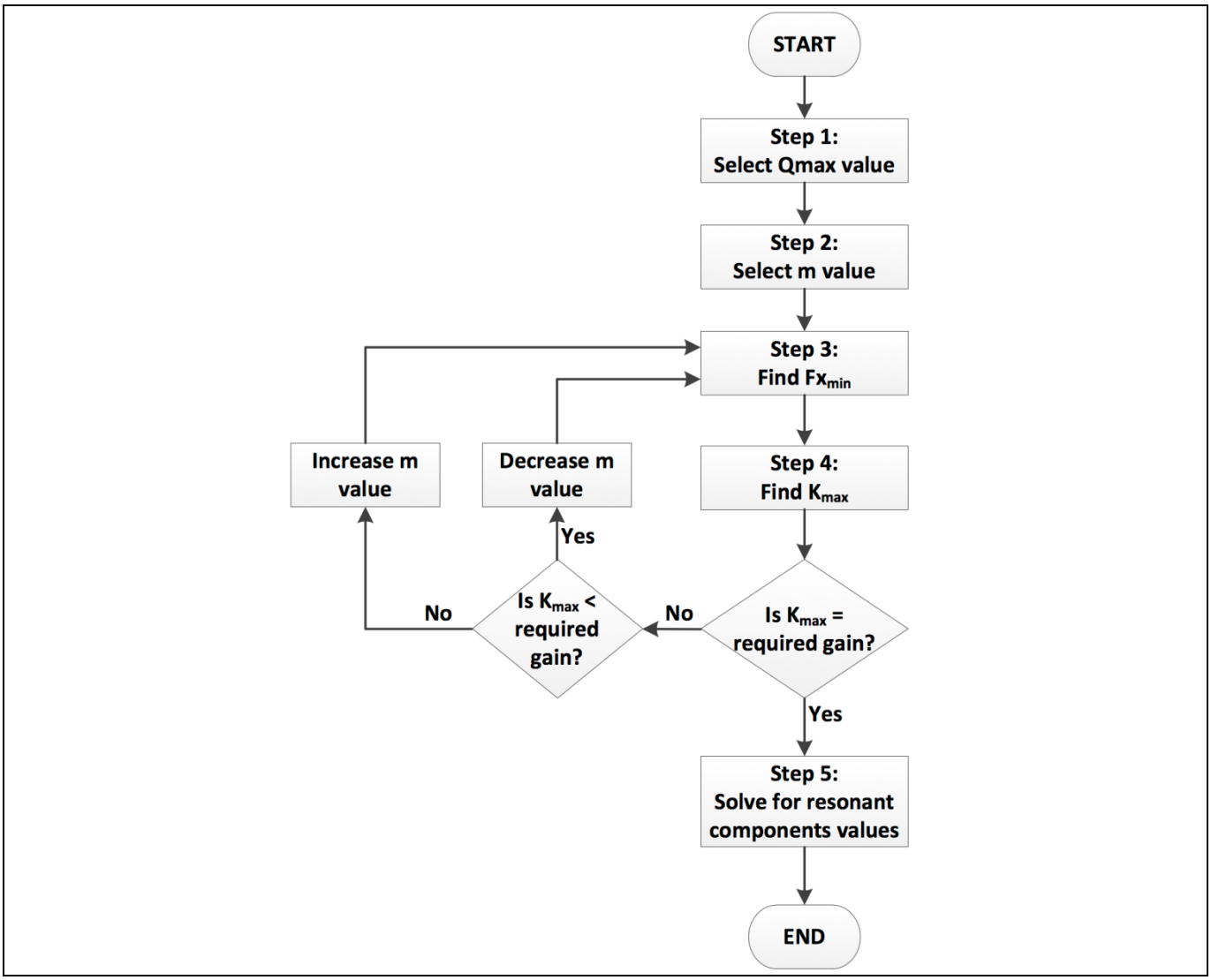


**Figure 13 Suggested FHA optimization process**

For all the details of this method, refer to [2].

## 3.4 Notes on the selection of the inductance factor (m)

The inductance factor, equation (2), has an important impact on the converter operation. Lower values of m achieve higher boost gain and a narrower range of frequency modulation, meaning more flexible control and regulation, which is valuable in applications with a very wide input voltage range.

On the other hand, this also means smaller values of $L_m$, which leads to high magnetizing current circulating in the primary side. This current does not contribute to the power transferred, but mainly generates conduction losses on the primary side.

In other words, there is a trade-off between flexible regulation and overall efficiency requirements, especially at light load.

In the case of the demo board described in this document, the main goal is to achieve high efficiency, so a relatively high m is selected. This minimizes the circulating current from the magnetizing inductance. This is permitted as the stated input range is relatively narrow, and a higher value of $L_m$ will be acceptable as long as sufficient current is available to achieve resonant transitions under light load conditions.

We rely on the bulk capacitor in the case of specific hold-up time requirements at the complete AC/DC SMPS level. However, high-density designs may not permit this, as the bulk capacitor does not reduce in size with increasing switching frequency. In some cases, adjustment of the input voltage range may be needed.

In this case, the chosen value is **m≈12**.

## 3.5 Resonant components calculation

Combining equations (1) and (2), we get a system where the unknown variables are $L_r$, $C_r$ and $L_m$.

Solving it means the following values are set for the LLC converter:

$$n = \frac{Np}{Ns} = \frac{V_{in_nom}}{2 \cdot V_{out_nom}} \approx 16 \Rightarrow Np = 16; Ns = 1 \quad (6)$$

$$m = \frac{Lr + Lm}{Lr} \approx 12 \Rightarrow Lm = 195\mu H; Lr = 17\mu H \quad (7)$$

$$Cr = 66nF \quad (8)$$

$$fr = \frac{1}{2\pi \cdot \sqrt{Lr \cdot Cr}} \approx 150KHz \quad (9)$$

## 3.6 ZVS behavior: energy and time considerations

The ZVS calculations involve two types of analysis, one in the energy domain and the other in the time domain. The goal is to have enough energy in the resonant tank to be able to discharge the output capacitance of the primary MOSFET, but also maintain an appropriate dead-time between the two devices.

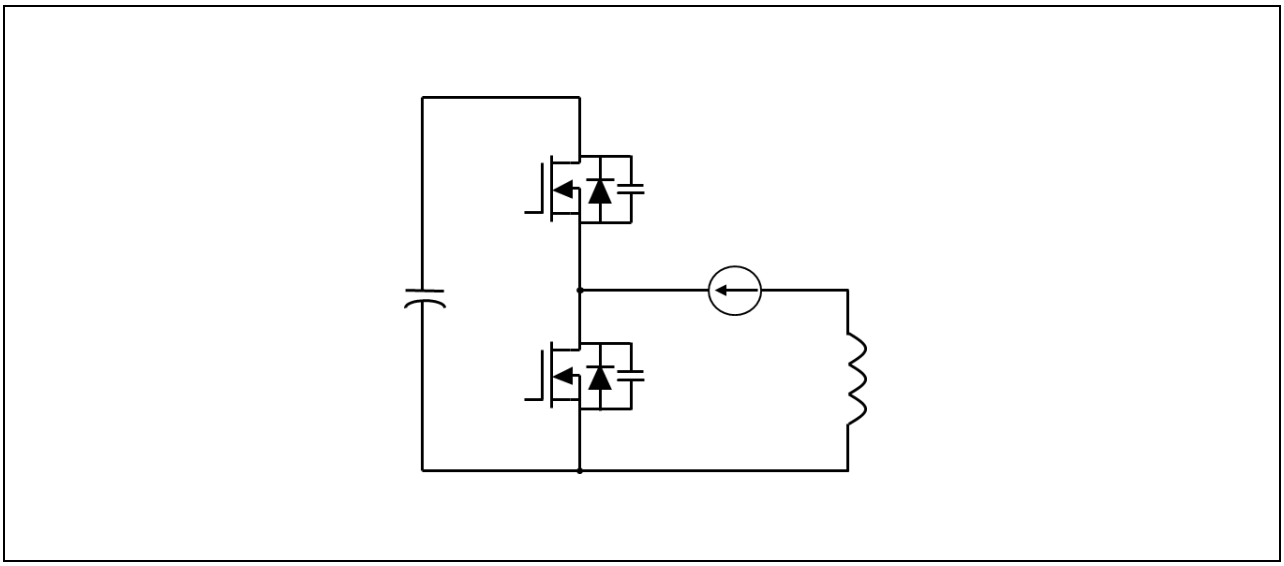

**Figure 14 Equivalent circuit in resonant drain-to-source transitions**

The two key parameters in our analysis are the following:

$C_{o(er)}$ is the $C_{oss}$ energy-related component of the HV MOSFET used, in this case IPP60R170CFD7.

$Q_{oss}$ is the charge stored in $C_{oss}$ at $V_{in(nom)}$ = 380 V DC. $Q_{oss}$ is linked to $C_{o(tr)}$ by the formula:

$Q_{oss} = C_{o(tr)} * V_{in(nom)}$

$C_{o(er)}$ and $C_{o(tr)}$ are the effective output capacitances of the MOSFET, respectively energy and time related.

### 3.6.1 Energy-related equations

$$I_{mag_min} = \frac{2\times\sqrt{2}}{p} \times \frac{n\times V_o}{2p\times f_{sw_max}\times L_m} = 0.672A \quad (10)$$

$$En_{res_min} = \frac{1}{2}\cdot(L_m + L_r)\cdot I^2_{mag_min} = 95.1\mu J \quad (11)$$

$$En_{cap_max} = \frac{1}{2}\cdot(2C_{o(er)})\cdot V^2_{DS_max} \approx 9\mu J \quad (12)$$

$$\Rightarrow En_{res_min} > En_{cap_max} \quad (13)$$

### 3.6.2 Time-related equations

It can be demonstrated that:

$$t_{dead} = \frac{t_{ecs}}{2} + \frac{2\cdot Q_{oss,\,@\,400V}}{I_{m,\,pk}} \quad (14)$$

where $t_{dead}$ is the dead-time set between the conduction time of the two HB devices and $t_{ecs}$ is the time when the channel of each MOSFET remains in conduction after turning it off (linear mode operation), which is a function of device parameters including $V_{gs(th)}$, $R_{g(tot)}$ and $C_{gs}/C_{gd}$.

Using the formula above, together with the minimum and maximum values of the magnetizing current and considering $t_{ecs}$ = 10 nsec:

$$I_{mag_min} = \frac{2\cdot\sqrt{2}}{\pi}\cdot\frac{n\cdot V_o}{2\pi\cdot f_{sw_max}\cdot L_m} = 0.672A \quad (10)$$

$$I_{mag_max} = \frac{2\cdot\sqrt{2}}{\pi}\cdot\frac{n\cdot V_o}{2\pi\cdot f_{sw_min}\cdot L_m} = 1.66A \quad (11)$$

$$t_{dead,\min} = \frac{t_{ecs}}{2} + \frac{2 \cdot Q_{oss,@400V}}{I_{m,ag,\max}} \approx 130 n\sec \quad (14)$$

$$t_{dead,\max} = \frac{t_{ecs}}{2} + \frac{2 \cdot Q_{oss,@400V}}{I_{m\,ag,\min}} \approx 311 n\sec \quad (15)$$

## 3.7 Main transformer design

The most critical condition for the main transformer is full load, mainly for thermal reasons. The selection of the core size and material is based on this condition along with the power density target (thereby including switching frequency) and the available airflow.

Keeping sufficient margin in the design, the minimum efficiency requirement at full load is fixed for the HB LLC converter at 97 percent, which means the goal is to keep the total dissipated power in that condition below 18 W.

In order to guarantee a balanced spread of power and heating, a good rule in the design of the LLC converter is to keep the total power dissipated in the main transformer below one-sixth of the total dissipated power, which means the maximum permitted power should be 3 W. This is our first important design input.

$$P_{trafo_MAX} = 3W \quad (16)$$

The maximum operating temperature is 55°C, as is typical for server applications. Due to the transformer safety isolation approvals, the maximum operating temperature of the transformer must be lower than 110°C, so:

$$\Delta T_{trafo_MAX} = (110 - 55)°C = 55°C \quad (17)$$

From (16) and (17) the maximum thermal resistance of the core shape can be easily derived:

$$R_{th_trafo_MAX} = \frac{\Delta T_{trafo_MAX}}{P_{trafo_MAX}} = \frac{55}{3} °C/W = 18.3°C/W \quad (18)$$

Our selected core shape must have a thermal resistance lower than 18.3°C/W.

This requirement can be fulfilled through various methods; the preferred one will allow for maximizing the ratio between available winding area and effective volume, in line with equation (18).

Also, considering the power density target (in the range of 20 W/inch$^3$), the most suitable selection is

PQ 35/35, shown in Figure 15.

The related coil former shows a minimum winding area of 1.58 cm$^2$ and a thermal resistance of 16.5°C/W. As this is lower than the result from (18), it is able to dissipate up to 3.33 W by keeping the $\Delta T_{MAX}$ less than 55°C.

Once it has been verified that the thermal equations are fulfilled, we can proceed with the design of the primary and secondary windings and the core material selection with some important goals:

- Fitting the geometry/overall dimensions of the core
- Fulfilling the condition in (16)

Try to split the losses between core and windings as equally as possible: ideally a 50:50 ratio should be achieved at full load, but any ratio close to it would be acceptable.

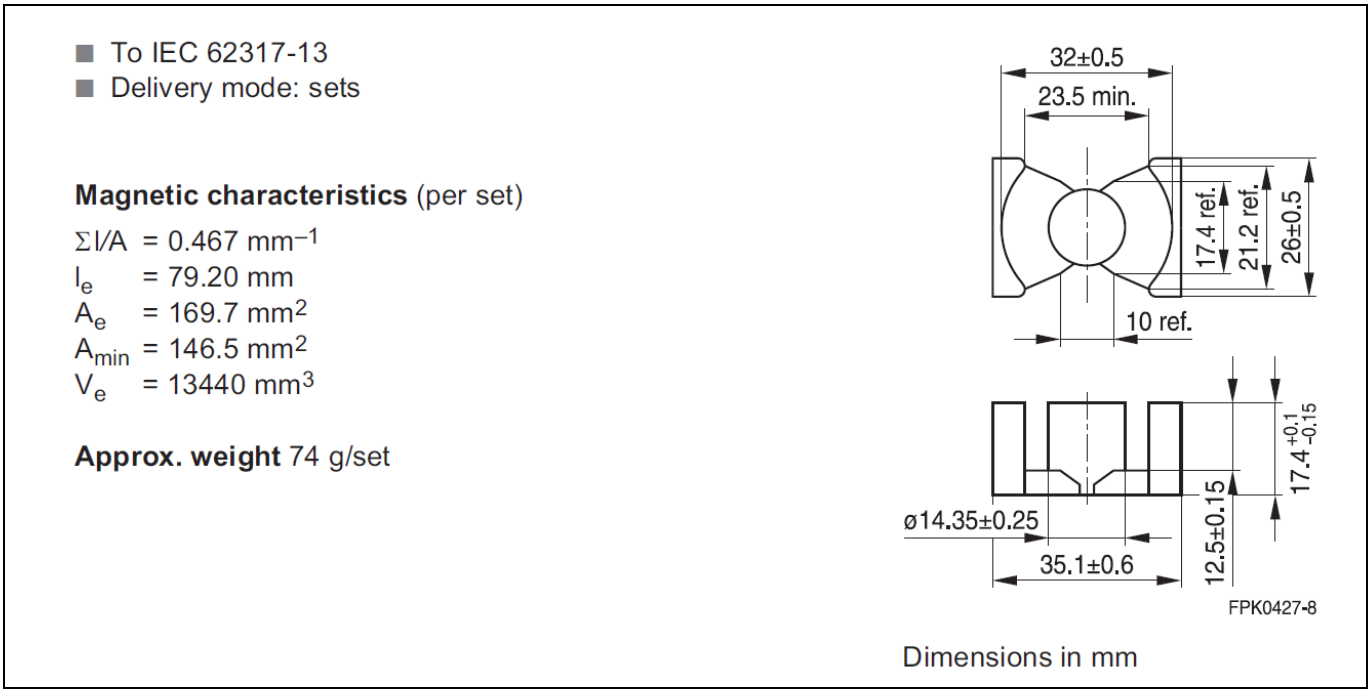


**Figure 15 TDK-Epcos PQ35/35 core**

The selected core material is the ferrite TDK PC95, showing a very interesting plot of core losses (PCV) vs flux density vs frequency (see Figure 16).

The final structure of the main transformer is shown in Figure 17, below. This has been developed in cooperation with the partner company Kaschke Components GmbH, of Göttingen, Germany.

The primary is realized using a “sandwich” technique with 16 turns of 4 layers of litz wire, 45 strands, 0.1 mm diameter. This minimizes the AC losses due to skin and proximity effects. The secondary is made with a 20 × 0.5 mm copper band.

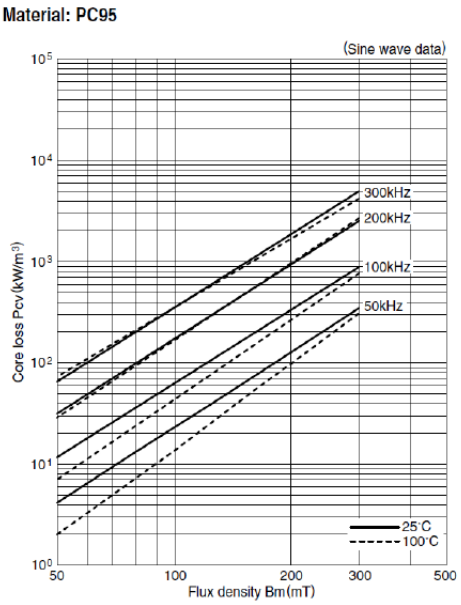


**Figure 16 Ferrite core material TDK PC95**

With this choice, at full-load condition, the total copper losses (primary + secondary, DC + AC components) are 1.1 W and the core losses are 1.8 W, so overall:

$$P_{trafo} = P_{copper} + P_{core} = 2.9W < P_{trafo_MAX} = 3W \quad (19)$$

In other words, equation (19) fulfils the thermal equation (18).

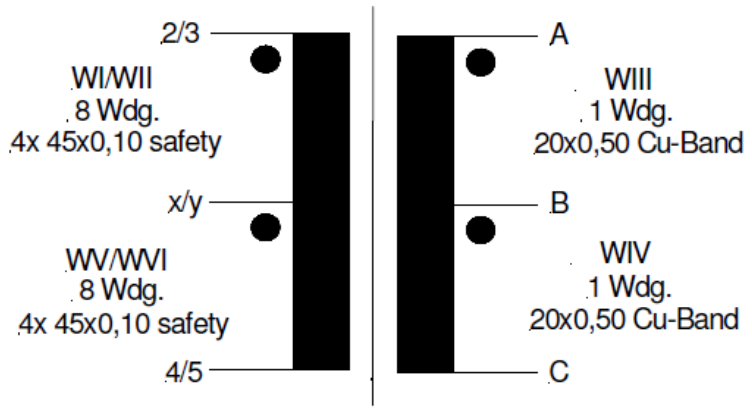


**Figure 17 Winding structure of the PQ 35/35 LLC transformer (Kaschke Components GmbH)**

An important transformer parameter involved in the LLC design is the primary or magnetizing inductance $L_m$, which, according to equation (7), must be 195 µH. This value is obtained with distributed air gap on the side

legs of the PQ core. This construction is preferred since it minimizes the effect of the “fringing flux” that generates additional losses in the windings close to the inner limb.

## 3.8 Resonant choke design

In LLC designs with stringent power density requirements, the resonant choke is normally embedded in the transformer as the leakage inductance is used for this purpose. This technique has the advantage of saving space and the cost of an additional magnetic component. It also has some drawbacks, including the challenge of controlling the value of $L_r$ in mass production.

In this design, it has been decided to use an external $L_r$. This is because the demo board is intended to be primarily used for testing and benchmarking, and high power density is not the main focus. Having the resonant inductance externally allows a more flexible way of changing the resonant tank.

According to equation (7), the overall value of $L_r$ shall be 17 µH, including the contribution of the transformer primary leakage inductance.

The external resonant choke is realized using an RM-12 core and a winding construction that is illustrated in Figure 18 below, and implemented by the partner company Kaschke Components GmbH.

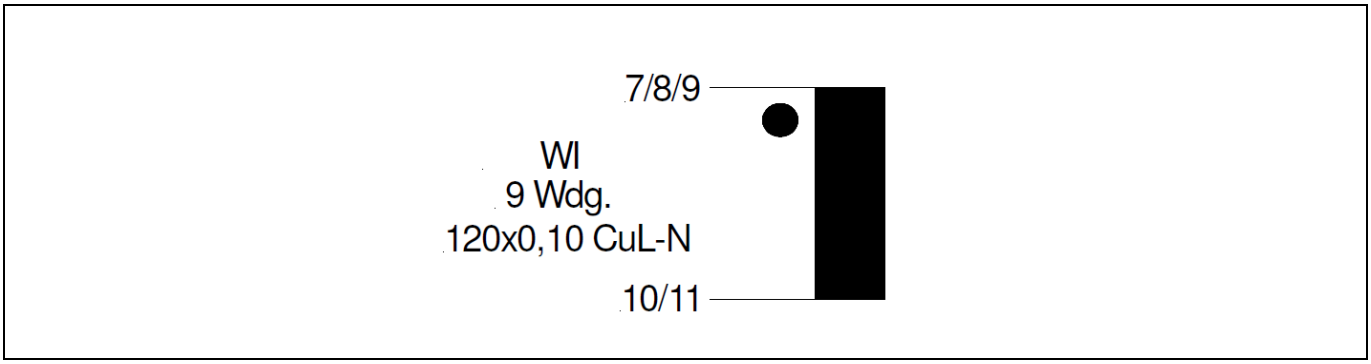


**Figure 18 Winding structure of the RM12 resonant choke (Kaschke Components GmbH)**

## 3.9 SR stage

In applications that target high efficiency at both low and high loads (such as 80Plus® Titanium), while often requiring high power densities, it is critical to select SR-stage MOSFETs that combine multiple key characteristics.

First of all, these SR MOSFETs should exhibit very low $R_{DS(on)}$. Indeed, due to the low voltages observed on the secondary side of server power supplies, large currents flow through the SR MOSFETs. Compared with other topologies such as ZVS PSFB, using the LLC topology leads to increased peak currents for the SR MOSFETs, as well as higher RMS currents $I_{RMS}$.

The conduction losses $P_{cond}$ of each SR MOSFET are given by:

$$P_{cond_SR} = R_{DS,on} \cdot (I_{RMS})^2 \quad (20)$$

These losses can only be mitigated through the use of a MOSFET with very low $R_{DS(on)}$.

Secondly, it is critical for these SR MOSFETs to exhibit low gate charges $Q_g$.

At light load, the switching losses of the SR MOSFETs dominate the conduction losses. For the LLC topology, the main contributor to these switching losses is $Q_g$.

Most of the time, a driving voltage of 12 V is applied to the SR MOSFETs. Although 12 V is not necessarily the optimized driving voltage, it is very popular in server PSUs because it is readily available. There is no need to derive it from another voltage rail. Therefore, we decided to follow this trend for the demo board by driving the SR MOSFETs with 12 V.

This requirement for low $Q_g$ gives MOSFET manufacturers additional challenges, especially considering that SR MOSFETs also need to exhibit a very low $R_{DS(on)}$. This was possible for Infineon due to the new Infineon OptiMOS™ 40 V generation, where the gate charges have been significantly reduced in comparison with the previous generation.

Thirdly, the paralleled SR MOSFETs should turn on almost simultaneously.

This can be achieved by tightening the voltage threshold $V_{GS(th)}$ range. For the new OptiMOS™ 40 V generation, the datasheet guarantees a very narrow $V_{GS(th)}$ range, with minimum and maximum values equal to 1.2 V and 2.0 V respectively.

Finally, the MOSFET package is critical for a variety of reasons.

The package should exhibit low parasitic inductances in order to confine its contribution to the $V_{DS}$ overshoot to a strict minimum. This is even more critical in server applications using the LLC topology, as the limited headroom for the $V_{DS}$ overshoot between the transformer secondary voltage (25 V) and the 90 percent derating (36 V maximum) or even 80 percent derating (32 V maximum) applied to the $V_{DS}$ of the SR MOSFETs;

Moreover, due to the conflicting requirements for high power density and high current capability, the package should combine a minimum footprint with good power dissipation.

Due to the high current densities arising at the source pins, which can lead to electromigration and destruction of the SR MOSFETs, the package should provide an enlarged source connection. While the first two points are addressed by standard SuperSO8 packages, it is the addition of source fused leads implemented in the new Infineon OptiMOS™ 40 V generation that reduces the high current densities mentioned above.

# 4 Board description

## 4.1 General overview

Figure 2 shows the top view, bottom view and assembly of the 600 W HB LLC demo board. Key components are: **(1)** heatsink assembly of primary-side switches IPP60R170CFD7, **(2)** resonant capacitor, **(3)** LLC analog controller ICE2HS01G, **(4)** resonant inductor, **(5)** main transformer, **(6)** PCB assembly of the auxiliary circuit with bias QR flyback controller ICE2QR2280Z, **(7)** heatsink assembly for cooling the SRs, **(8)** output capacitors, **(9)** output inductor, **(10)** HB MOSFET gate driver 2EDL05N06PFG, **(11)** SR OptiMOS™ BSC010N04LS and **(12)** dual-channel gate driver 2EDN7524F used for SR MOSFETs.

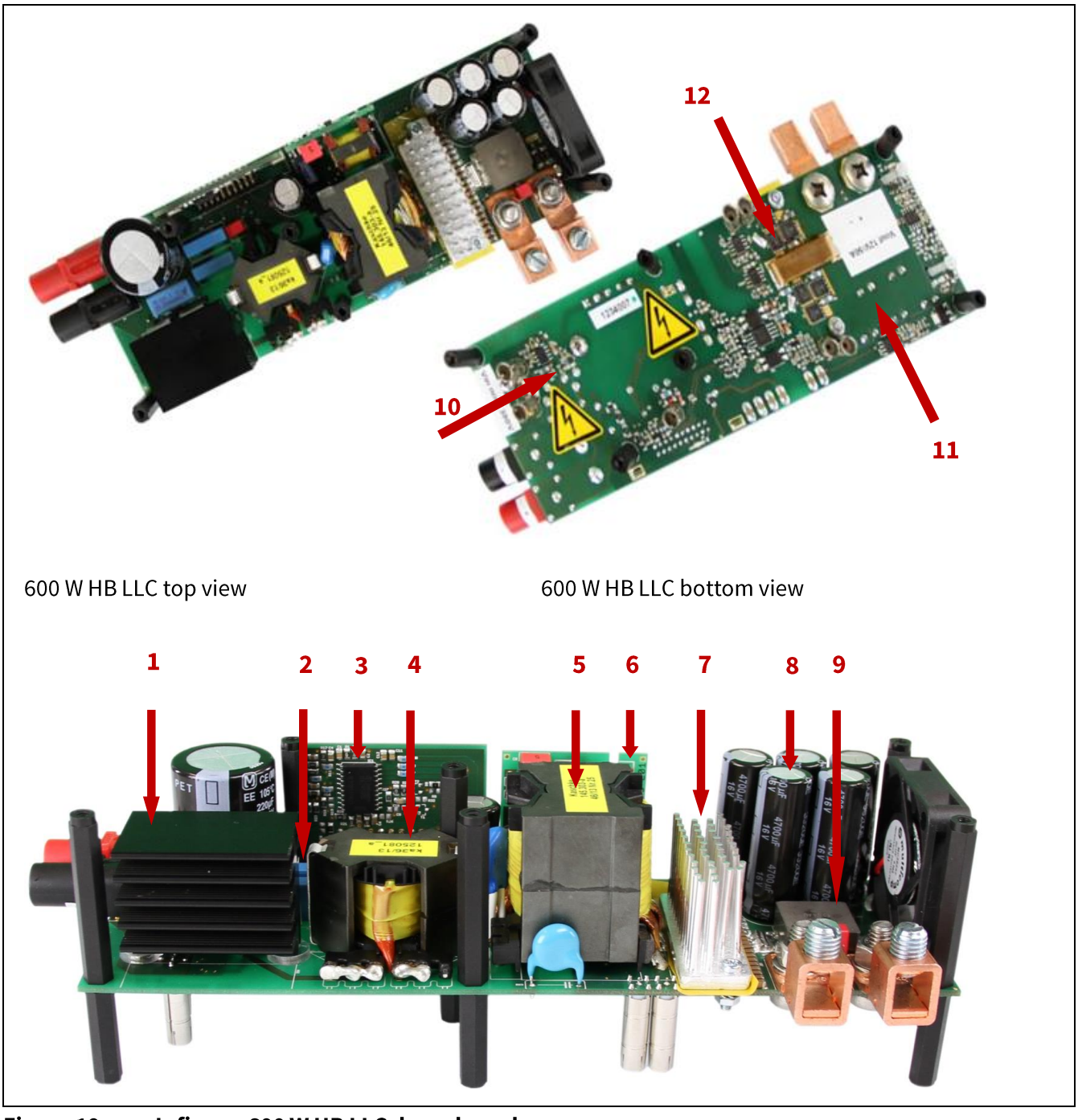


**Figure 19 Infineon 600 W HB LLC demo board**

## 4.2 Infineon components used in the board

This 600 W HB LLC demo board is a full Infineon solution meeting the highest efficiency standard, 80Plus® Titanium, using the following parts:

### 4.2.1 Primary HV MOSFETs 600 V CoolMOS™ CFD7

CoolMOS™ is a revolutionary technology for HV power MOSFETs, designed according to the SJ principle and pioneered by Infineon Technologies. The latest 600 V CoolMOS™ CFD7 is the successor to the 650 V CoolMOS™ CFD2 series and is an optimized platform tailored to target soft-switching applications such as PSFB (ZVS) and LLC. Resulting from reduced gate charge ($Q_g$), best-in-class reverse recovery charge ($Q_{rr}$) and improved turn-off behavior, the 600 V CoolMOS™ CFD7 offers the highest efficiency in resonant topologies. As part of Infineon's fast body diode portfolio, this new product series blends all the advantages of a fast-switching technology together with superior hard-commutation robustness, without sacrificing easy implementation in the design-in process. The 600 V CoolMOS™ CFD7 technology meets the highest efficiency and reliability standards and furthermore supports high power density solutions. Altogether, 600 V CoolMOS™ CFD7 makes resonant switching topologies more efficient, more reliable, lighter and cooler.

Features:

- Ultra-fast body diode
- Low gate charge ($Q_g$)
- Best-in-class reverse recovery charge ($Q_{rr}$)
- Improved MOSFET reverse diode dv/dt and di/dt ruggedness
- Lowest FOM $R_{DS(on)}$*$Q_g$ and $R_{DS(on)}$*$E_{oss}$
- Best-in-class $R_{DS(on)}$ in SMD and THD packages
- Qualified for industrial-grade applications according to JEDEC (J-STD20 and JESD22)

Benefits:

- Excellent hard-commutation ruggedness
- Highest reliability for resonant topologies
- Highest efficiency with outstanding ease-of-use/performance trade-off
- Enabling increased power density solutions

Applications:

- Suitable for soft-switching topologies
- Optimized for PSFB (ZVS), LLC stages in server, telecom and EV charging applications

### 4.2.2 LLC analog controller ICE2HS01G

ICE2HS01G is Infineon's second-generation HB LLC controller designed specifically for high-efficiency HB or FB LLC resonant converters with SR control for the secondary side. With its new driving techniques, SR can be realized for LLC converters operated with secondary switching current in both CCM and DCM conditions. No special SR controller IC is required on the secondary side. Maximum switching frequency is supported up to 1 MHz. Apart from the patented SR driving techniques, this IC provides a very flexible design and also integrates full protection functions. It is adjustable for maximum/minimum switching frequency, soft-start time and frequency, dead-time between primary switches, and turn-on and turn-off delay for the secondary SR MOSFETs. The integrated protections include input voltage brown-out, primary three-level over-current, secondary over-load protection and no-load regulation. It also includes a burst mode function, which offers an

operation with low quiescent current maintaining high efficiency at low output load while keeping output ripple voltage low.

### 4.2.3 HB gate driver 2EDL05N06PFG

Developers of consumer electronics and home appliances strive continuously to achieve higher efficiency in applications and smaller form factors. One area of interest in power supply design is the switching behavior and power losses of new power MOSFETs, such as the latest generations of CoolMOS™ with dramatically reduced gate charges, as they can be optimized by dedicated driver ICs.

The 2EDL05N06PFG IC is one of the drivers from Infineon's 2EDL EiceDRIVER™ compact 600 V HB gate driver IC family with a monolithic, integrated, low-ohmic and ultra-fast bootstrap diode. Its level shift SOI technology supports higher efficiency and smaller form factors within applications. Based on the SOI technology, there is excellent ruggedness for transient voltages. No parasitic thyristor structures are present in the device. Hence, no parasitic latch-up will occur at any temperature or voltage condition. The outputs of the two independent drivers are controlled at the low-side using two different CMOS resp. LS TTL compatible signals, down to 3.3 V logic. The device includes an Under Voltage (UV) detection unit with a hysteresis characteristic, which is optimized for either IGBTs or MOSFETs. 2EDL05N06PF (DSO-8) and 2EDL05N06PJ (DSO-14) are driver ICs with Under Voltage Lockout (UVLO) for MOSFETs. These two parts are recommended for server/telecom SMPS, LV drives, e-Bike, battery charger and HB-based SMPS topologies.

### 4.2.4 Advanced dual-channel gate driver 2EDN7524F

The fast dual-channel 5 A non-isolated gate driver is an advanced dual-channel driver optimized for driving both standard and SJ MOSFETs, as well as gallium nitride (GaN) power devices, in all applications in which they are commonly used. The input signals are TTL compatible with an HV capability up to 20 V and down to -5 V. The unique ability to handle -5 V DC at the input pins protects the IC inputs against GND bounce transients.

Each of the two outputs is able to sink and source current up to 5 A, utilizing a true rail-to-rail stage, which ensures very low impedances of 0.7 Ω up to the positive rail and 0.55 Ω down to the negative rail. Very low channel-to-channel delay matching (typically 1 ns) is implemented, which enables the double source-and-sink capability of 10 A by paralleling both channels.

Different logic input/output configurations guarantee high flexibility for all applications; e.g. with two paralleled switches in a boost configuration. The gate driver is available in three package options: PG-DSO-8, PG-VDSON-8 and PG-TSDSO-8-X (size-minimized DSO-8).

Main features

- Industry-standard pin-out
- Two independent low-side gate drivers
- 5 A peak sink-to-source output driver at $V_{DD}$ = 12 V
- True low-impedance rail-to-rail output (0.7 Ω and 0.5 Ω)
- Enhanced operating robustness due to high reverse current capability
- -10 V DC negative input capability against GND bouncing
- Very low propagation delay (19 ns)
- Typ. 1 ns channel-to-channel delay matching
- Wide input and output voltage range up to 20 V
- Active low output driver even on low power or disabled driver
- High flexibility through different logic input configurations
- PG-DSO-8, PG-VDSON-8 and TSSOP-8 package

- Extended operation from -40°C to 150°C (junction temperature)
- Particularly well suited to driving standard MOSFETs, SJ MOSFETs, IGBTs or GaN power transistors

### 4.2.5 Bias QR flyback controller ICE2QR2280Z

ICE2QRxxxx is a second-generation QR PWM CoolSET™ with a power MOSFET and start-up cell in a single package optimized for off-line power-supply applications such as LCD TVs, notebook adapters and auxiliary/housekeeping converters in SMPS. The digital frequency reduction with decreasing load enables a QR operation down to very low load. As a result, the average system efficiency is significantly improved compared to conventional solutions. The Active Burst Mode (ABM) operation enables ultra-low power consumption in standby mode operation and low output voltage ripple. The numerous protection functions give full protection of the power supply system in failure modes. The main features of the ICE2QR2280Z that make it suitable as an auxiliary converter for this LLC demo board are:

- HV (650 V/800 V) avalanche rugged CoolMOS™ with start-up cell
- QR operation
- Load-dependent digital frequency reduction
- ABM for light-load operation
- Built-in HV start-up cell
- Built-in digital soft-start
- Cycle-by-cycle Peak Current Limitation (PCL) with built-in Leading Edge Blanking (LEB) time
- Foldback point correction with digital sensing and control circuits
- $V_{CC}$ UV and Over Voltage Protection (OVP) with auto-restart mode
- Over-load/open-loop protection with auto-restart mode
- Built-in over-temperature protection with auto-restart mode
- Adjustable output OVP with latch mode
- Short winding protection with latch mode
- Maximum on-time limitation
- Maximum switching period limitation

### 4.2.6 SR MOSFETs OptiMOS™ BSC010N04LS

For the SR stage, the selected device is BSC010N04LS, from the latest OptiMOS™ 40 V family. SR is naturally the best choice for high-efficiency LLC designs with low output voltage and high output current, as in this demo board. In applications that target high efficiency at both light and heavy loads – such as 80Plus® Titanium – while often requiring high power densities, it is critical to select SR MOSFETs that combine following key characteristics:

- Very low $R_{DS(on)}$: BSC010N04LS provides the industry's first 1 m Ω 40 V product in a SuperSO8 package
- Low gate charge, $Q_g$, which is important in order to minimize driving losses, with benefits for light-load efficiency
- Very tight $V_{GS(th)}$ range: when paralleling this allows the MOSFETs to turn on almost simultaneously. Selected OptiMOS™ offer very close minimum and maximum values of $V_{GS(th)}$, respectively 1.2 V and 2 V
- Monolithically integrated Schottky-like diode, to minimize associated conduction losses

- Package; the BSC010N04LS in SuperSO8 with source-fused leads is able to address all of the typical crucial requirements for a suitable SR MOSFET package:
  - Minimizing parasitic inductances
  - Combining compact footprint with good power dissipation
  - Enlarged source connection in order to minimize the occurrence of electromigration

## 4.3 Board schematics

### 4.3.1 Main board schematic

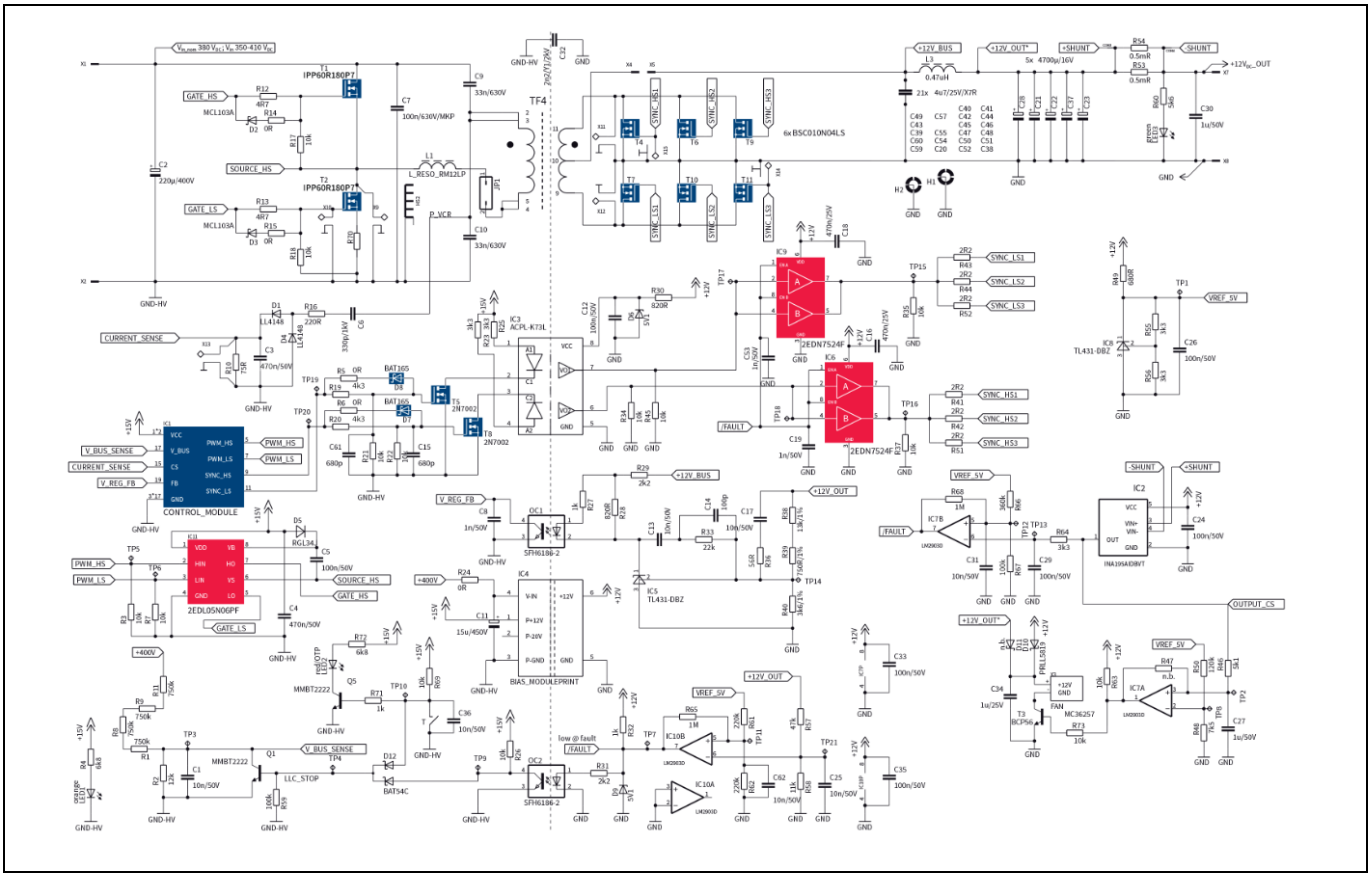

**Figure 20 Main board schematic**

### 4.3.2 Controller board schematic

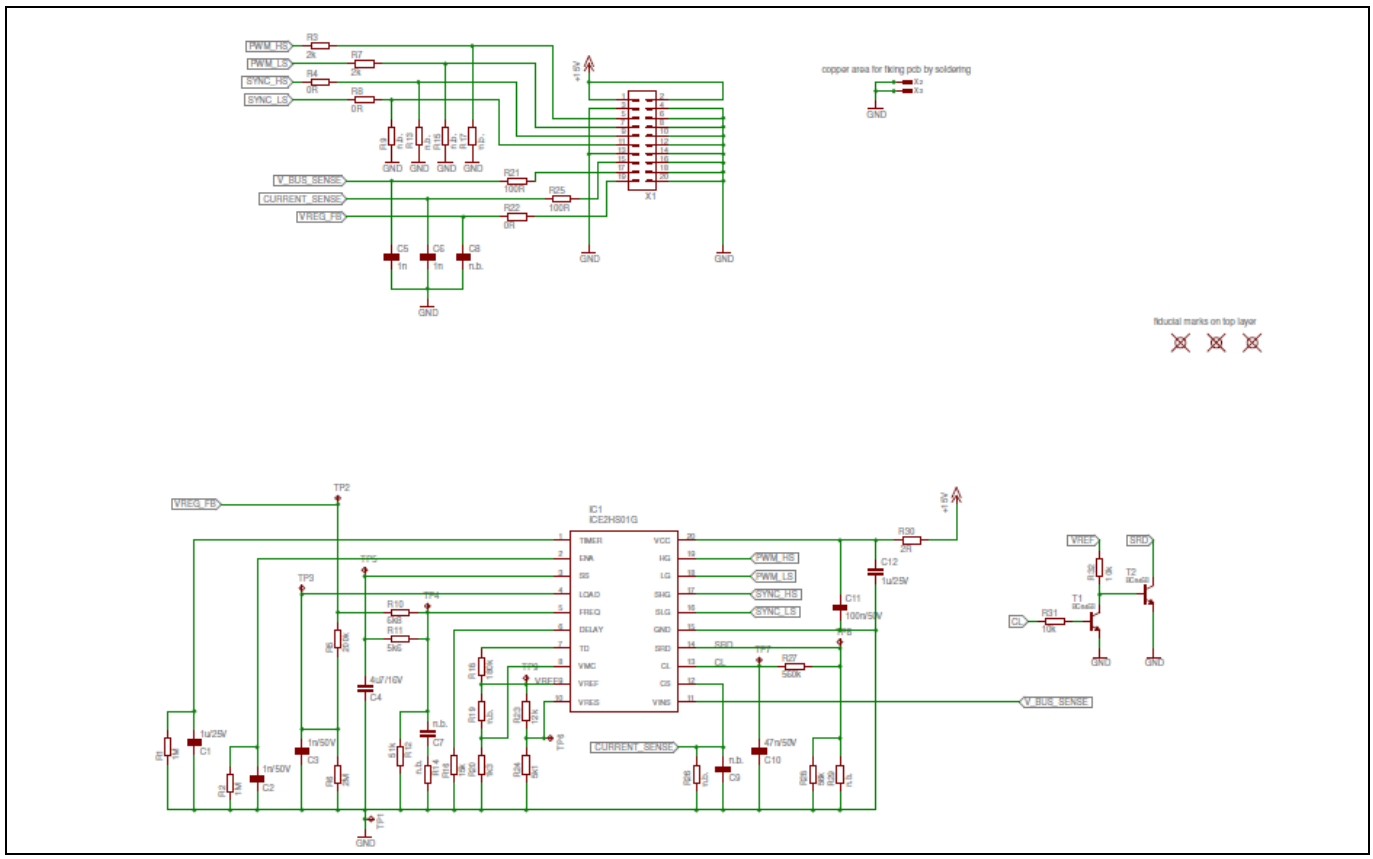


**Figure 21 Controller board schematic**

### 4.3.3 Bias board schematic

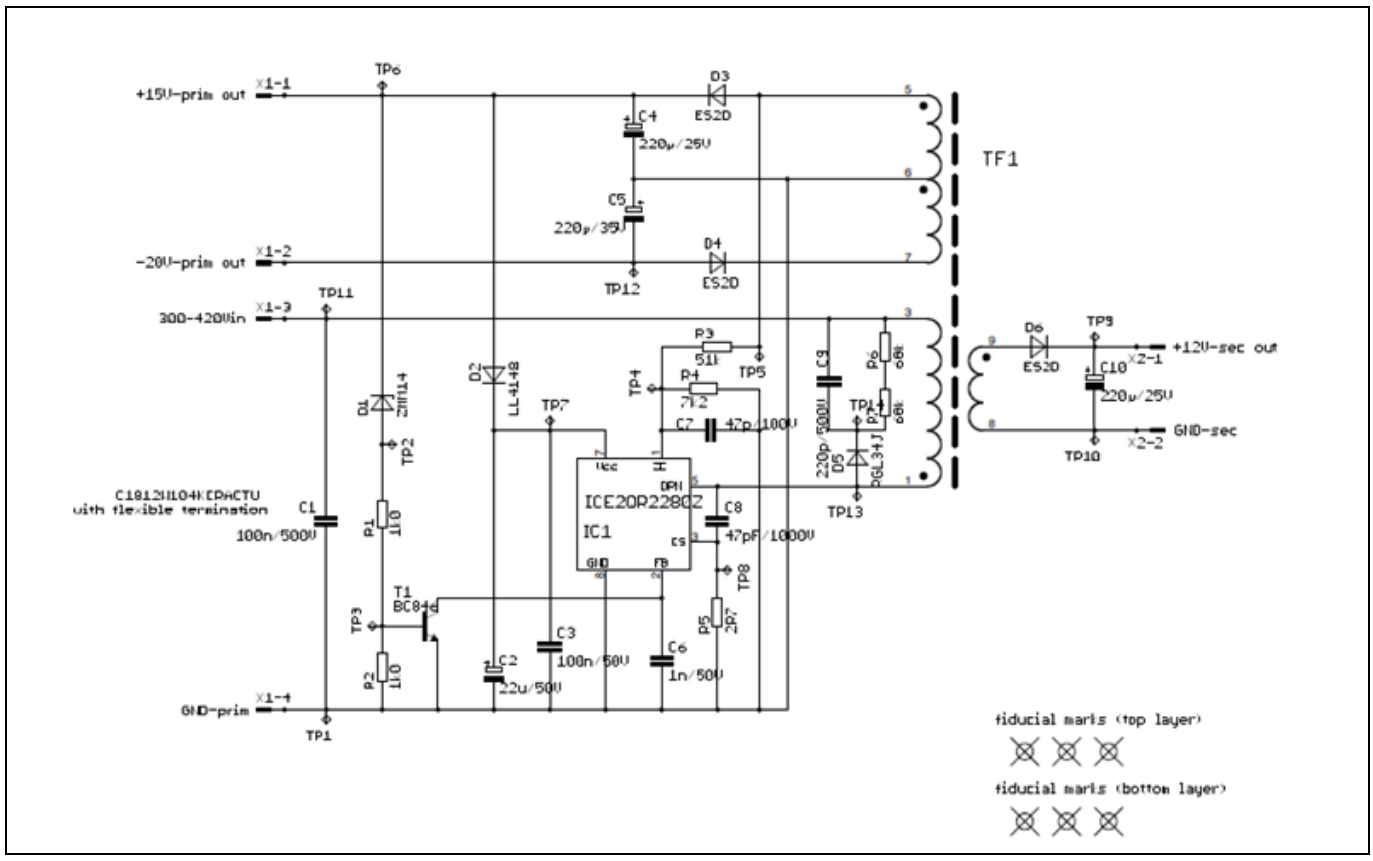


**Figure 22 Bias board schematic**

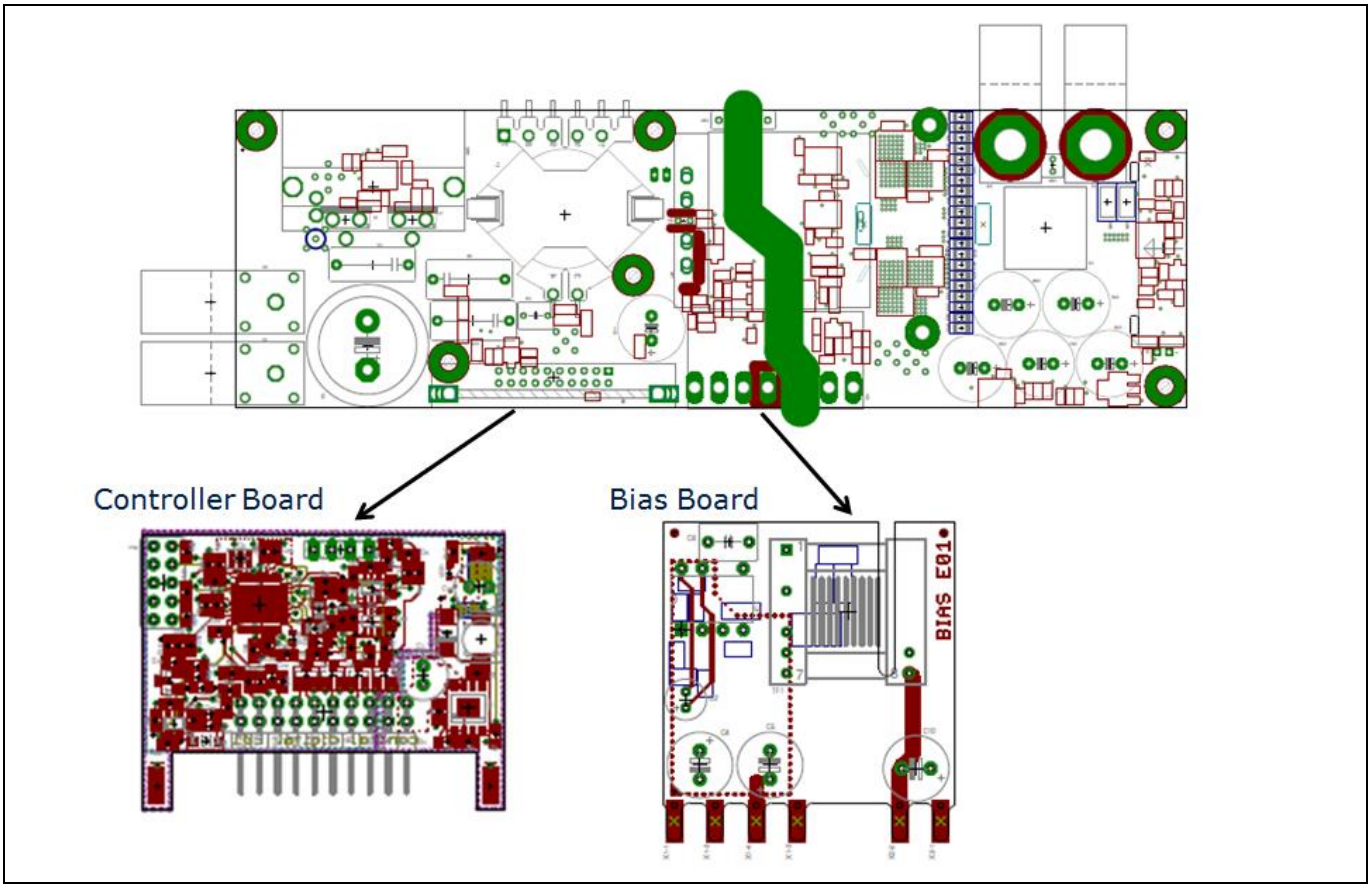


**Figure 23 Main board PCB with controller – and bias board**

## 4.4 Critical LLC operation – hard commutation

In LLC converters, hard commutation of the body diode can occur during start-up, burst mode, over-load and short-circuit conditions. This condition can be prevented during design by using a proper control technique, a correct selection of resonant components and a proper setting of the minimum and maximum operating frequency. Hard commutation occurs in LLC converters during the commutation period of the body diode. During this time, resonant inductor current is flowing through the body diode of the MOSFET, creating a ZVS condition upon this MOSFET's turn-on. When the current is not able to change its direction prior to the turn-on of the other MOSFET, more charge will be stored in the P-N junction of that MOSFET. When the other MOSFET turns on, a large shoot-through current will flow due to the reverse recovery current of the body diode. This results in a high reverse recovery peak current $I_{RRM}$ and high reverse recovery dv/dt, which could sometimes lead to MOSFET breakdown. This operation is widely explained in technical literature [5, 7].

In the 600 W HB LLC analog-controlled demo board, only the burst mode condition (described in detail later) tends to lead to hard commutation.

The event shown in Figure 24 was captured only once during a start-up in burst mode operation, and this is not easy to reproduce.

In fact, the drain current in the low-side MOSFET is not able to change direction, thus inducing hard commutation during the turn-off of the high-side switch. However, the $V_{DS_peak}$ is 474 V, so within the 80 percent derating even during this abnormal condition, despite the huge current spike. In addition, $V_{GS_MAX}$ is only 23.2 V – well below the allowed datasheet limit. We can conclude that the IPP60R170CFD7 is able to withstand this condition without any problem.

In fact, the fast body diode feature intrinsically reduces the probability of hard commutation, and the stress in general on the device during that event.




**Figure 24 Hard commutation during burst mode operation, $V_{DS_pk}$, $V_{GS_max/min}$ and $I_{DS_MAX}$**

For the sake of completeness, it should be stated that in a broad range of applications the voltage spike on the gate and drain may vary depending on the layout quality and parasitics. In some cases, a different selection of turn-on and turn-off gate resistors may be needed in order to keep $V_{GS}$ and $V_{DS}$ within an acceptable range. Even a possible $R_g$ change in the range of ±10 Ω will not significantly affect the efficiency, due to the 600 V CoolMOS™ CFD7 technology switching behavior.

It is important to highlight that the condition described in Figure 24 is the real worst case we have been able to capture in the 600 W HB LLC demo board using analog control. There are no other observed hard-commutation events during start-up, nor during output short-circuit conditions.

## 4.5 ZVS behavior analysis

The converter achieves nearly full ZVS at turn-on, already at 10 percent output load (5 A), as shown in Figure 25. ZVS is of course guaranteed across the entire load range.

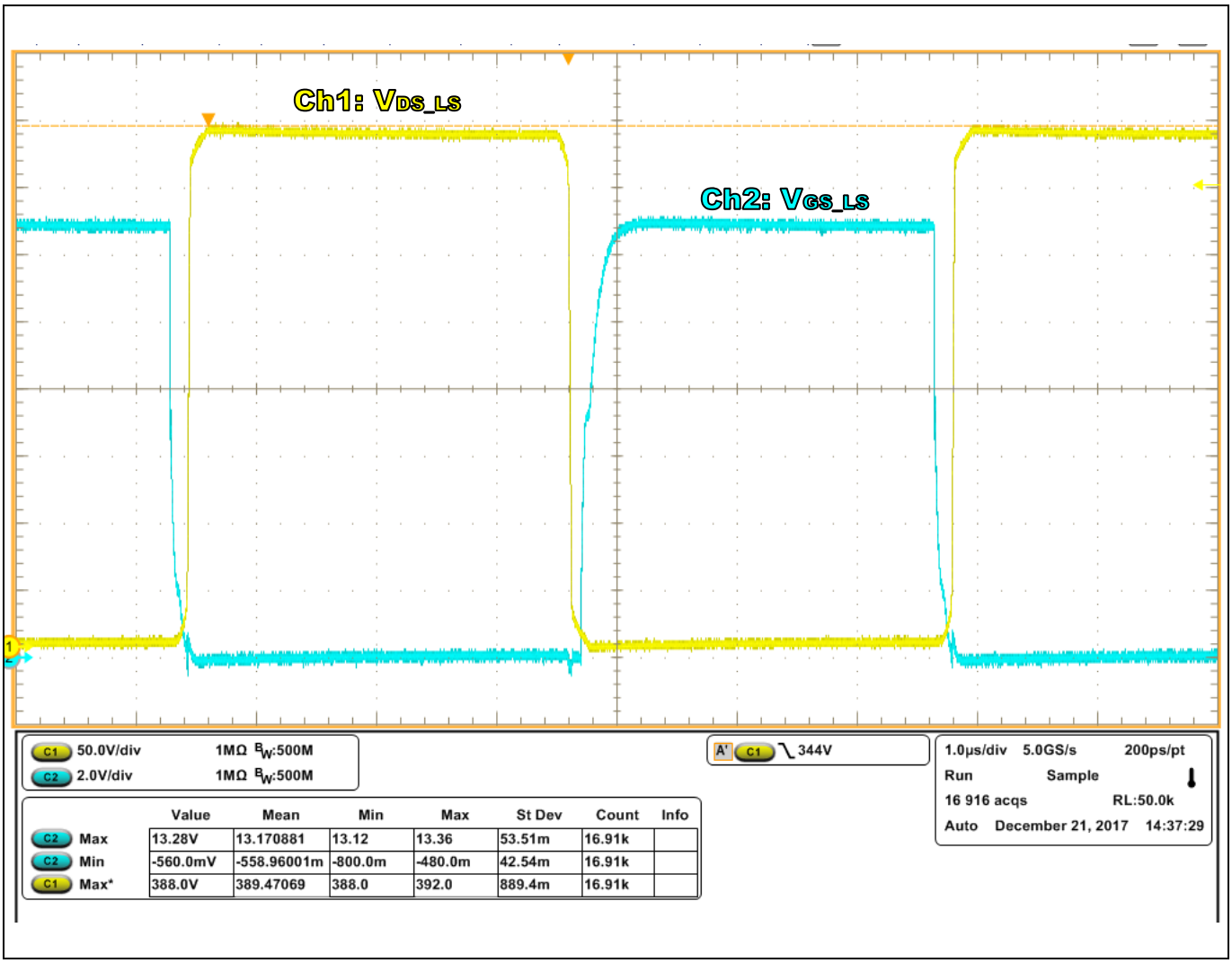


**Figure 25 Nearly full ZVS starting at 5 A load**

## 4.6 Burst mode operation

At no-load or very light-load condition, the LLC controller provides a frequency approaching its maximum setting. In this condition, in order to achieve full ZVS, the magnetizing current should be high enough to discharge the output capacitances. Due to the magnetizing current limitation, switching loss (especially turn-off loss) is relatively high if the devices continue to switch at the highest frequency. In order to overcome this phenomenon, the burst mode function is enabled and implemented. This results in lower switching losses and driving losses, due to the low burst frequency.

Additionally, this helps to achieve regulation even in a no-load condition, preventing challenges often seen in LLC converters in that condition. These regulation problems are typically due to parasitic components such as the primary-to-secondary main transformer coupling capacitance and the SR MOSFET's output capacitance. The combination of these factors generates the third resonant frequency in the LLC gain curve, making the

converter virtually uncontrollable at no-load. The burst mode overcomes this problem, by limiting the unwanted primary-to-secondary power transfer, due to these parasitic effects.

For further details about this operation of the LLC converter, please refer to the specific literature [8].

The waveforms in Figure 26 illustrate the burst mode technique applied in our 600 W HB LLC demo board.

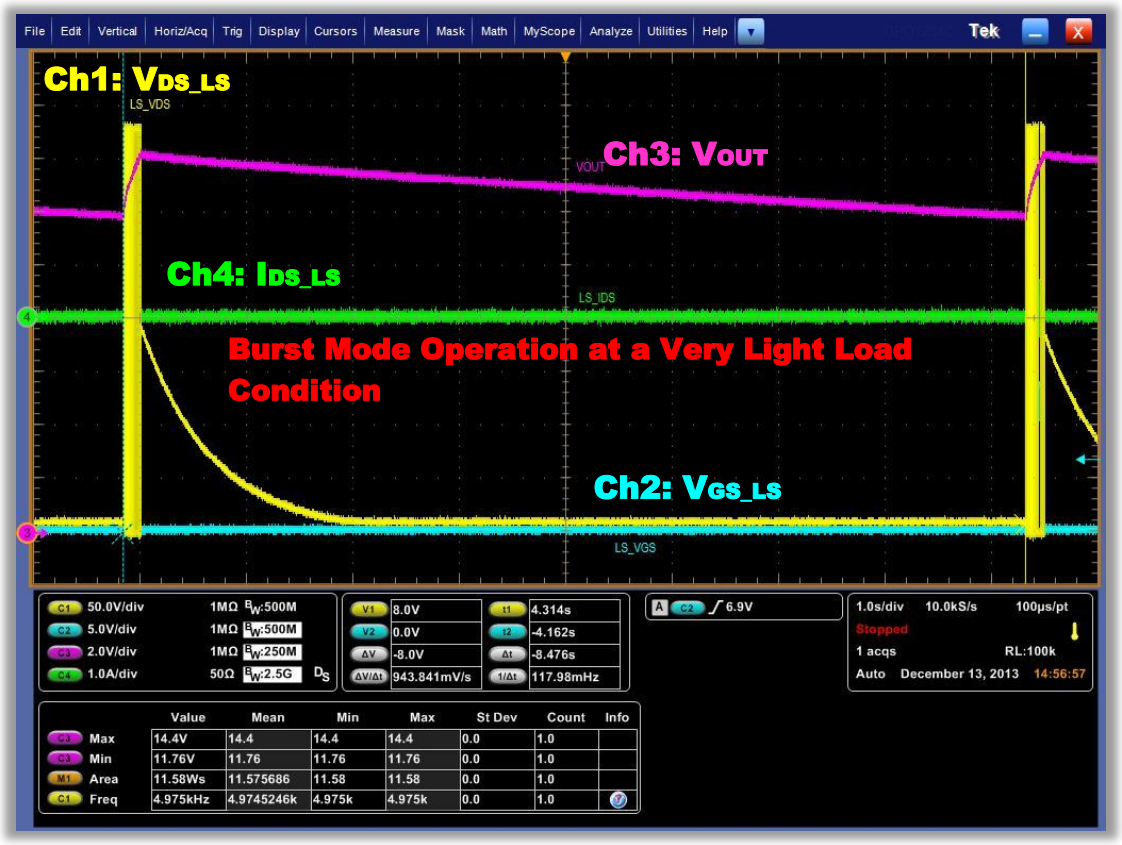


**Figure 26 Burst mode operation at no-load and very light-load condition**

## 4.7 Efficiency

### 4.7.1 80Plus® Titanium efficiency target

Figure 27 shows the efficiency measurement performed on the 600 W HB LLC demo board using an IPP60R170CFD7 with reference to the 80Plus® Titanium standard efficiency (dotted blue line). The 80Plus® Titanium standard fixes the minimum efficiency requirement at the three most important load conditions in a computing/server application, 10 percent, 50 percent and 100 percent.

The combination of proper converter design (including the resonant tank and transformer) and HV device selection enables meeting (with a reasonable margin) the efficiency targets, especially in the 10–40 percent load range.

Proper selection of LV SR devices and secondary-side design influences the performance more in the 40–100 percent load range.

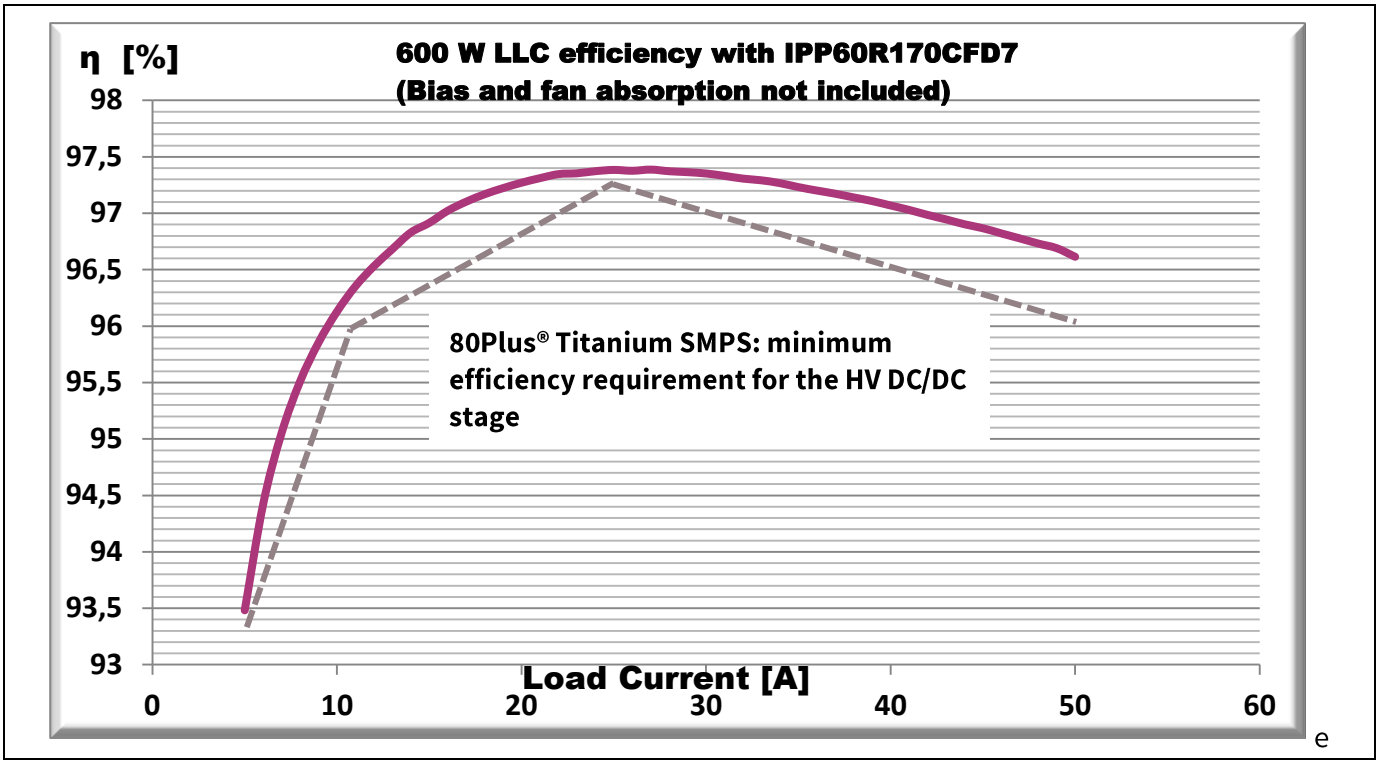


**Figure 27** **Infineon CFD7-based 600 W HB LLC demo board efficiency vs 80Plus® Titanium standard efficiency**

The measurement is performed in a fully automated set-up, as shown in Figure 28, according to the guidelines included in [9]. The total accuracy of the measurement chain is in the ±0.1 percent range.

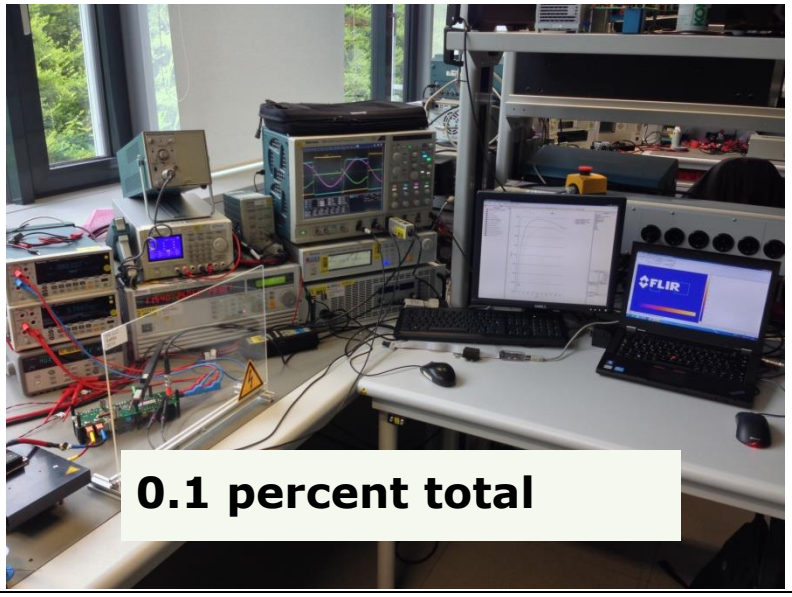


**Figure 28** **Infineon 600 W HB LLC automated efficiency measurement set-up**

### 4.7.2 Losses breakdown

Along with the efficiency plot shown in the previous paragraph, it is interesting to analyze the losses breakdown between the different components of the demo board. Figures 29, 30 and 31 below provide this overview.

The contribution of the primary MOSFETs progressively increases from light to heavy load. On the other hand, the contribution of the main transformer is important at 10 percent load, but it tends to decrease at higher loads. This is mainly due to the core losses (higher at light load due to higher switching frequency) and the magnetizing inductance, which is almost constant and independent of the load. In fact, this feature allows the HB LLC topology to easily achieve ZVS down to very light load and differentiates the HB LLC topology from other soft-switching approaches, such as the ZVS PSFB.

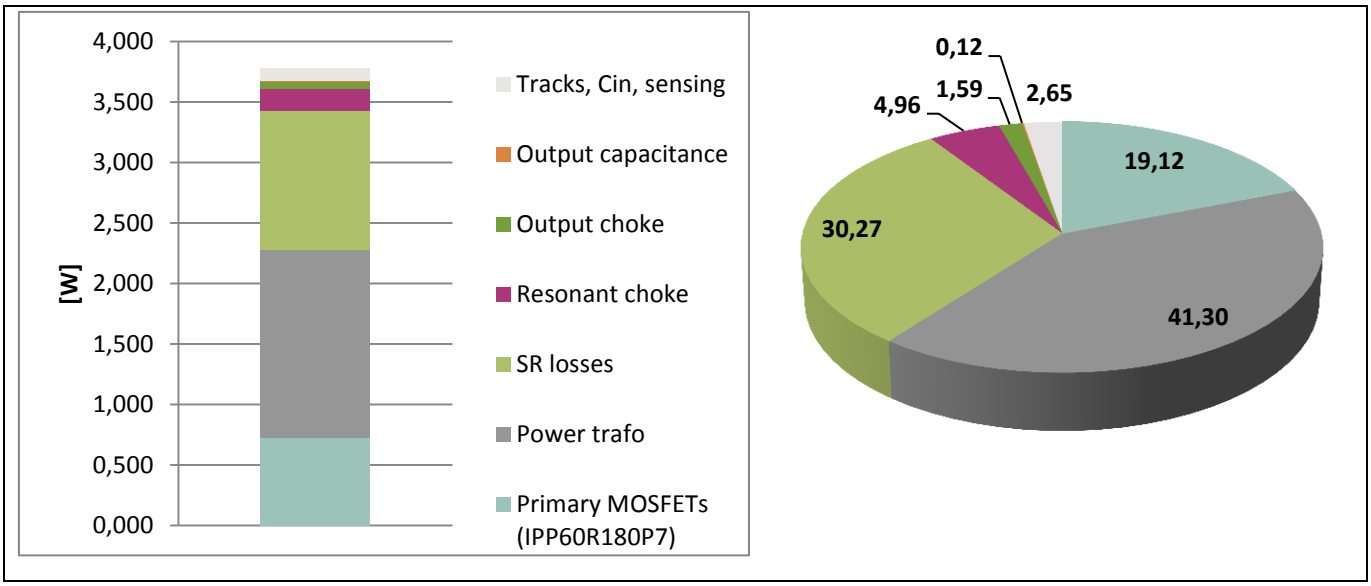


**Figure 29 10 percent $P_{max}$ overall load losses breakdown**

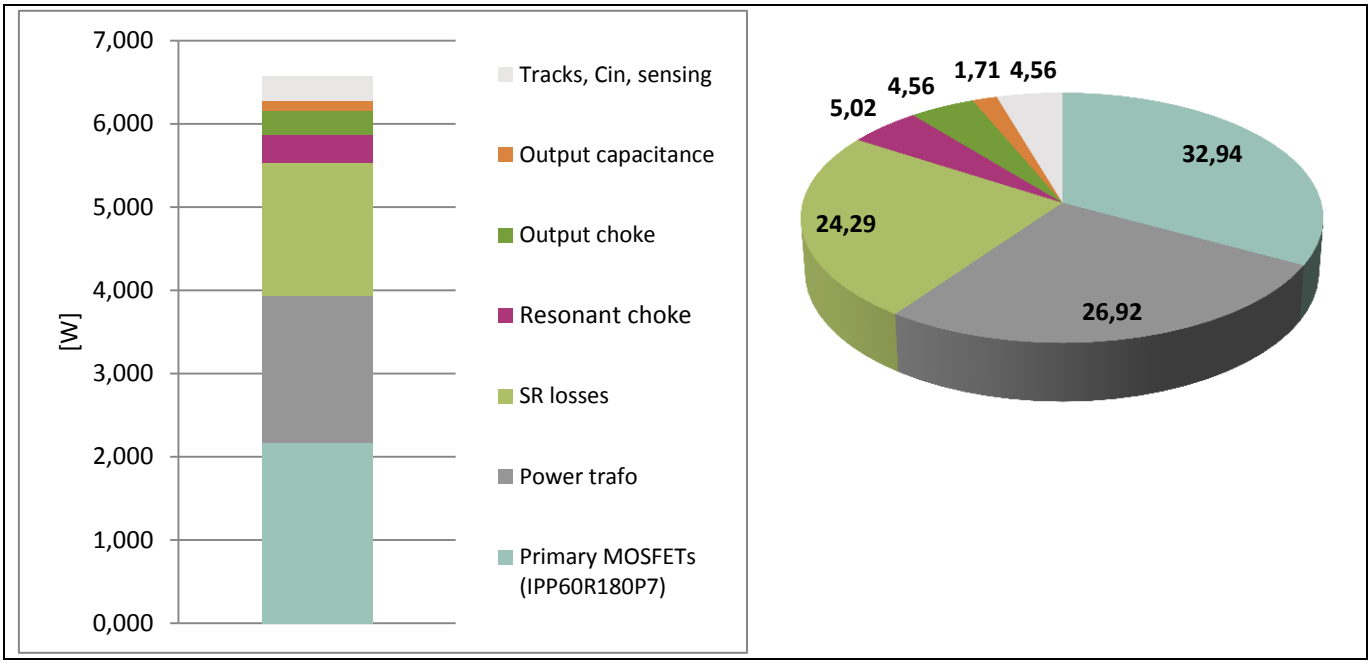


**Figure 30 50 percent $P_{max}$ overall load losses breakdown**

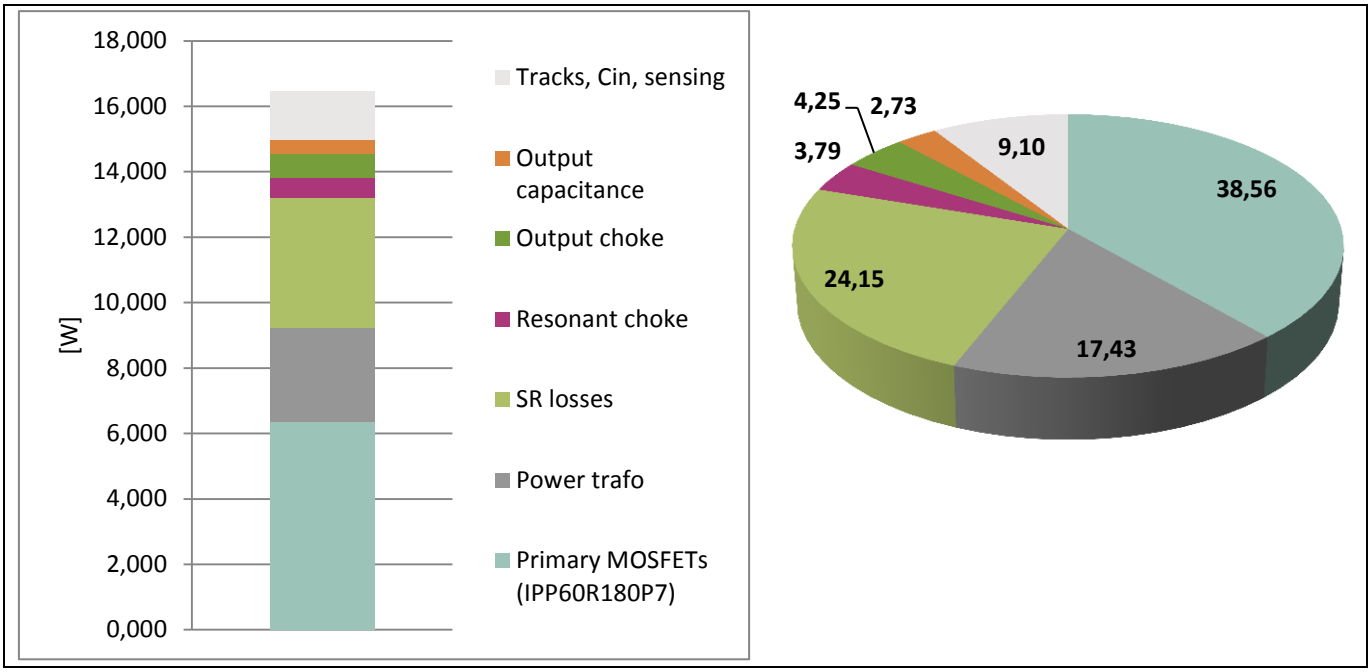


**Figure 31 100 percent $P_{max}$ overall load losses breakdown**

# 5 Conclusion

This document has described the 600 W HB LLC demo board, its principle of operation and its concept, along with the most important choices made in its design.

It has been demonstrated that the proper selection of primary HV MOSFETs and secondary MV MOSFETs in the SR stage, along with suitable design of the transformer and resonant tank and a control technique that achieves a level of efficiency for the HV DC-DC stage are necessary to be able to fulfill the 80Plus® Titanium standard at the complete PSU level.

The features of the new 600 V CoolMOS™ CFD7 have been deployed through a valuable application example provided by our board.

Specifically, the excellent switching FOM, due to the reduced gate charge and turn-off losses, is the key enabler for the very high efficiency down to 10 percent load, as per 80Plus® Titanium requirements.

The low typical $R_{DS(on)}$ is the main reason why CFD7 shows high efficiency in the range 50–100 percent load, where the conduction losses are the predominant HV MOSFET loss mechanism in the HB LLC topology.

Moreover, the ruggedness of the CFD7 technology with fast body diode has been demostrated in some of the HB LLC critical operating conditions, where the primary HV MOSFETs are submitted to heavy stress, especially in designs where the converter control (e.g. analog) is not able to prevent these unpredictable events.

# 6 Test/power-up procedure

| Test | Test procedure | Condition |
|---|---|---|
| **1. Auxiliary circuit turn-on** | Apply 30 V on the input | $V_{in}$: ~30 V |
| | | Orange LED will light up |
| **2. LLC converter turn-on** | Apply 350 V , converter will give $V_{out}$ = 12 V | $V_{in}$: 350 V |
| | | $V_{out}$: 12 V |
| **3. Operational switching frequency** | Using a voltage probe, monitor switching frequency at the following test conditions: | $V_{in}$: 380 V |
| | | $V_{out}$: 12 V |
| | 5 A output load 10 percent load – ~ 155 kHz* | $I_{out}$: 5 A |
| | 25 A output load 50 percent load – ~ 142 kHz* | $I_{out}$: 25 A |
| | 50 A output load 100 percent load – ~ 132 kHz* | $I_{out}$: 50 A |
| | (*measure frequency at “Pri_LS_VGS” – connector; +-10 kHz) | |
| **4. Fan enable** | Switch the load from 50 A to 5 A. Increase the output load current from 11–14 A, fan should turn on | $V_{in}$ = 380 V |
| | | $I_{out}$ = 5 A |
| | | Fan is off |
| | | $V_{in}$ = 380 V |
| | | $I_{out}$ = 11-14 A |
| | | Fan is on |
| **5. Switch off input start-up at no load** | Switch off the input | $V_{in}$ = 0 V |
| | | $I_{out}$ = 0 A |
| | Switch at 380 Vat **no-load output**. Operation should be in burst mode | $V_{in}$ = 380 V |
| | | $I_{out}$ = 0 A |
| | | $V_{out}$ = 11.5–12.5 |
| **6. Switch off input start-up at full load** | Switch off the input | $V_{in}$ = 0 V |
| | | $I_{out}$ = 0 A |
| | Apply 380V with full load at 50 A output. $V_{out}$ is between 11.8 Vand 12.2 V * (*measure on the board connector) | $V_{in}$ = 380 V |
| | | $V_{out}$: 11.8–12.3 V |
| | | $I_{out}$ = 50 A |
| **7. Running no load -> output short-circuit** | Switch off load from 380 V **50 A** to 380 V **0 A** | $V_{in}$ = 380 V |
| | Short-circuit the load using the short-circuit function of the e-load. **Converter should latch** | (after short-circuit) **$V_{out}$ = 0V** |
| | | $I_{out}$ = 0 A |
| **8. Switch off input and remove short-circuit** | Switch off the input | $V_{in}$ = 0 V |
| **9. Running full load -> over-current protection** | Remove short-circuit function on the load | $I_{out}$ = 0 A |
| | Apply 380 V 50 A with full-load output. Increase the current on the output 1 A each step until the converter goes into protection starting from 50 A. OCP occurs between 55 A and 62 A | $V_{in}$ = 380 V |
| | | $I_{out}$ = 50 A |
| | | OCP = between 55 A and 62 A |
| **10. Running full load -> output short-circuit** | Apply 380 V 50 A with full-load output. Short-circuit the load using the short-circuit functions of the load. Converter should latch | $I_{out}$ = 0 A |
| | | $V_{in}$ = 380 V |
| | | $I_{out}$ = 50 A |
| | | (after short-circuit) **$V_{out}$ = 0 V** |
| **11. Switch off input; start-up -> output short-circuit** | Switch off the input | $V_{in}$ = 0 V |
| | | $I_{out}$ = 0 A |

| | | |
|---|---|---|
| | Apply 380 V with output load short-circuit. Converter should be in hiccup/latch mode | $V_{in}$ = 380 V |
| | | $I_{out}$ = short-circuit |
| | | $V_{out}$ = 0 V short-circuit (hiccup/latch) |
| **12. Switch off input and remove short-circuit** | Switch off the Input | $V_{in}$ = 0 V |
| | Remove short-circuit function on the load | $I_{out}$ = 0 A |
| **13. Dynamic loading** | Apply 380 V . Set the electronic load to dynamic loading mode with the following settings: | $V_{in}$ = 380 V |
| | CCDH1: $I_{out}$ 5 A | $I_{out}$ = 5–50 A |
| | CCDH2: $I_{out}$ 50 A | $V_{out}$ = 11.5–12.5 V |
| | Dwell time: 10 ms | |
| | Load slew rate: 1 A/µs | |

# 7 Useful materials and links

The following links provide more detailed information about the Infineon devices used, and the magnetic components.

- Primary HV MOSFETs CoolMOS™ IPP60R170CFD7
  www.infineon.com/600v-CFD7
- LLC analog controller ICE2HS01G
  http://www.infineon.com/dgdl/ICE2HS01G_PDS_v2.1_20110524_Public.pdf?folderId=db3a30441 2b4079501 12b408e8c90004&fileId=db3a30432a40a650012a458289712b4c
- HB gate drive 2EDL05N06PFG
  http://www.infineon.com/dgdl/Infineon-2EDL05x06xx-DS-v02_05-EN.pdf?fileId=db3a30433e30e4bf013e3c649ffd6c8b
- Advanced dual-channel gate drive 2EDN7524F
  http://www.infineon.com/dgdl/Infineon-2EDN752x_2EDN852x-DS-v01_00-EN.pdf?fileId=5546d4624cb7f111014d672f9fbb5142
- Bias QR flyback controller ICE2QR2280Z
  http://www.infineon.com/dgdl/Datasheet_ICE2QR2280Z_v21_20110830.pdf?folderId=db3a304412b4079501 12b408e8c90004&fileId=db3a30432a7fedfc012a8d8038e00473
- SR MOSFETs OptiMOS™ BSC010N04LS
  http://www.infineon.com/dgdl/BSC010N04LS_rev2.0.pdf?folderId=db3a304313b8b5a60113cee8763b02d7&fileId=db3a3043353fdc16013552c1c63647c4
- Main transformer and resonant choke ferrite cores
  http://en.tdk.eu/blob/519704/download/2/ferrites-and-accessories-data-book-130501.pdf

# 8 References

[1] T. Fujihira: “Theory of Semiconductor Superjunction Devices”, Jpn. J. Appl. Phys., vol. 36, pp. 6254–6262, 1997

[2] F. Di Domenico, J. Hancock, A. Steiner, J. Catly, P. Yelamos, A. Medina: “600 W Halfbridge LLC eval board with 600 V CoolMOS™ C7 and digital control by XMC™”, Infineon Technologies, May 2016

[3] Sam Abdel Rahman: “Resonant LLC Converter: Operation and Design: 250 W 33 $V_{in}$ 400 $V_{out}$ Design Example”, Infineon Technologies, 2012

[4] Alois Steiner, Francesco Di Domenico and others: “600 W Half-Bridge LLC Evaluation Board with 600 V CoolMOS™ C7”, Infineon Technologies, 2015

[5] Lawrence Lin, Gary Chang: “Consideration of Primary-side MOSFET Selection for LLC topology”, Infineon Technologies, 2014

[6] Liu Jianwei, Li Dong: “Design Guide for LLC Converter with ICE2HS01G”, Infineon Technologies, July 2011

[7] Francesco Di Domenico, David Meneses Herrera, Stefano de Filippis: “3kW dual-phase LLC demo-board using 600 V CoolMOS™ CFD7 and digital control by XMC4400”, Infineon Technologies, 2017

[8] Jae-Hyun Kim, Chong-Eun Kim and others: “Analysis for LLC Resonant Converter Considering Parasitic Components at Very Light Load Condition”, 8th International Conference on Power Electronics, Korea, 2011

[9] Dr. Arshad Mansoor, Brian Fortenbery, Peter May-Ostendop and others: “Generalized Test Protocol for Calculating the Energy Efficiency of Internal AC-DC and DC-DC Power Supplies”, Revision 6.7, March 2014

# 9 List of abbreviations

BOM……Bill of Materials
$C_{GD}$ ……Internal gate drain capacitance
$C_{iss}$……Input capacitance
$C_{o(er)}$ …… Effective output capacitance
$C_r$ ……Resonant capacitance
di/dt ……Steepness of current slope at turn-off/turn-on
DUT ……Device Under Test
dv/dt ……Steepness of voltage slope at turn-off/turn-on
$E_{off}$……Energy losses at switch-off
$E_{on}$……Energy losses at switch-on
$E_{oss}$……Stored energy in output capacitance ($C_{oss}$) at typ. $V_{DS}$ = 400 V
FHA……First Harmonic Approximation
FOM……Figure of Merit
$f_r$ ……Resonant frequency
$I_D$…… Drain current
$I_{RMS}$……Effective root mean square current
$I_{mag}$ ……Magnetizing current
$I_{m,pk}$……Peak magnetizing current
K…… Gain factor
$L_r$ ……Resonant inductance
$L_m$……Magnetizing inductance
m…… Inductance factor
$N_p$ …… Primary winding
$N_S$……Secondary winding
n ……Transformer turn ratio
MOSFET……Metal Oxide Semiconductor Field Effect Transistor
$P_{cond_SR}$ ……Synchronous rectification conduction losses
PFC……Power Factor Correction
PNP…… Bipolar transistor type (pnp vs. npn)
$Q_{OSS}$ ……Charge stored in the $C_{OSS}$
Q ……Quality factor
$R_{ac}$……Total equivalent AC resistor
$R_{DS(on)}$……Drain-source on-state resistance
$R_{g,tot}$ ……Total gate resistor
$R_o$ ……Output resistor
$R_{th}$ ……Thermal resistance
$t_{dead}$……Dead-time
$t_{ecs}$ ……Early channel shut-down time
$V_{DS}$ ……Drain-to-source voltage
$V_{gs,th}$……Drain-to-source threshold voltage
$V_{In_AC}$ ……Input voltage, alternating current
$V_{In_nom}$ ……Nominal input voltage
$V_{out_nom}$……Nominal output voltage
ZCS……Zero Current Switching
ZVS……Zero Voltage Switching

## Revision history

### Major changes since the last revision

| Page or reference | Description of change |
|---|---|
| -- | First release |
| | |
| | |

**Trademarks of Infineon Technologies AG**
µHVIC™, µIPM™, µPFC™, AU-ConvertIR™, AURIX™, C166™, CanPAK™, CIPOS™, CIPURSE™, CoolDP™, CoolGaN™, COOLiR™, CoolMOS™, CoolSET™, CoolSiC™, DAVE™, DI-POL™, DirectFET™, DrBlade™, EasyPIM™, EconoBRIDGE™, EconoDUAL™, EconoPACK™, EconoPIM™, EiceDRIVER™, eupec™, FCOS™, GaNpowIR™, HEXFET™, HITFET™, HybridPACK™, iMOTION™, IRAM™, ISOFACE™, IsoPACK™, LEDrivIR™, LITIX™, MIPAQ™, ModSTACK™, my-d™, NovalithIC™, OPTIGA™, OptiMOS™, ORIGA™, PowIRaudio™, PowIRStage™, PrimePACK™, PrimeSTACK™, PROFET™, PRO-SIL™, RASIC™, REAL3™, SmartLEWIS™, SOLID FLASH™, SPOC™, StrongIRFET™, SupIRBuck™, TEMPFET™, TRENCHSTOP™, TriCore™, UHVIC™, XHP™, XMC™

Trademarks updated November 2015

**Other Trademarks**
All referenced product or service names and trademarks are the property of their respective owners.

**Edition 2018-01-12**

**Published by**

**Infineon Technologies AG**

**81726 Munich, Germany**

**© 2018 Infineon Technologies AG. All Rights Reserved.**

**Do you have a question about this document?**

**Email:** erratum@infineon.com

**Document reference**
**AN_1801_PL52_1801_180456**

**IMPORTANT NOTICE**

The information contained in this application note is given as a hint for the implementation of the product only and shall in no event be regarded as a description or warranty of a certain functionality, condition or quality of the product. Before implementation of the product, the recipient of this application note must verify any function and other technical information given herein in the real application. Infineon Technologies hereby disclaims any and all warranties and liabilities of any kind (including without limitation warranties of non-infringement of intellectual property rights of any third party) with respect to any and all information given in this application note.

The data contained in this document is exclusively intended for technically trained staff. It is the responsibility of customer's technical departments to evaluate the suitability of the product for the intended application and the completeness of the product information given in this document with respect to such application.

For further information on the product, technology, delivery terms and conditions and prices please contact your nearest Infineon Technologies office (**www.infineon.com**).

**WARNINGS**

Due to technical requirements products may contain dangerous substances. For information on the types in question please contact your nearest Infineon Technologies office.

Except as otherwise explicitly approved by Infineon Technologies in a written document signed by authorized representatives of Infineon Technologies, Infineon Technologies' products may not be used in any applications where a failure of the product or any consequences of the use thereof can reasonably be expected to result in personal injury.